

ฟลูออเรสเซนซ์คีโมเซ็นเซอร์ชนิดใหม่ฐานเฟอร์โรซีน



นางสาวพรชนก จินะแปง

จุฬาลงกรณ์มหาวิทยาลัย

CHULALONGKORN UNIVERSITY

วิทยานิพนธ์นี้เป็นส่วนหนึ่งของการศึกษาตามหลักสูตรปริญญาวิทยาศาสตรมหาบัณฑิต

สาขาวิชาเคมี ภาควิชาเคมี

คณะวิทยาศาสตร์ จุฬาลงกรณ์มหาวิทยาลัย

ปีการศึกษา 2556

ลิขสิทธิ์ของจุฬาลงกรณ์มหาวิทยาลัย

บทคัดย่อและแฟ้มข้อมูลฉบับเต็มของวิทยานิพนธ์ตั้งแต่ปีการศึกษา 2554 ที่ให้บริการในคลังปัญญาจุฬาฯ (CUIR)

เป็นแฟ้มข้อมูลของนิสิตเจ้าของวิทยานิพนธ์ ที่ส่งผ่านทางบัณฑิตวิทยาลัย

The abstract and full text of theses from the academic year 2011 in Chulalongkorn University Intellectual Repository (CUIR) are the thesis authors' files submitted through the University Graduate School.

NEW FERROCENE-BASED FLUORESCENT CHEMOSENSOR

Miss Pondchanok Chinapang



จุฬาลงกรณ์มหาวิทยาลัย

CHULALONGKORN UNIVERSITY

A Thesis Submitted in Partial Fulfillment of the Requirements
for the Degree of Master of Science Program in Chemistry

Department of Chemistry

Faculty of Science

Chulalongkorn University

Academic Year 2013

Copyright of Chulalongkorn University

Thesis Title	NEW FERROCENE-BASED FLUORESCENT CHEMOSENSOR
By	Miss Pondchanok Chinapang
Field of Study	Chemistry
Thesis Advisor	Associate Professor Paitoon Rashatasakhon, Ph.D.
Thesis Co-Advisor	Associate Professor Mongkol Sukwattanasinitt, Ph.D.

Accepted by the Faculty of Science, Chulalongkorn University in Partial
Fulfillment of the Requirements for the Master's Degree

.....Dean of the Faculty of Science
(Professor Supot Hannogbua, Dr.rer.nat.)

THESIS COMMITTEE

.....Chairman
(Associate Professor Vudhichai Parasuk, Ph.D.)

.....Thesis Advisor
(Associate Professor Paitoon Rashatasakhon, Ph.D.)

.....Thesis Co-Advisor
(Associate Professor Mongkol Sukwattanasinitt, Ph.D.)

.....Examiner
(Associate Professor Supason Wanichwecharungruang, Ph.D.)

.....Examiner
(Assistant Professor Patchanita Thamyongkit, Ph.D.)

.....External Examiner
(Gamolwan Tumcharern, Ph.D.)

พรชนก จินะแปง : ฟลูออเรสเซนต์เคมีโม่เซ็นเซอร์ชนิดใหม่ฐานเฟอร์โรซีน. (NEW FERROCENE-BASED FLUORESCENT CHEMOSENSOR) อ.ที่ปรึกษาวิทยานิพนธ์
 หลัก: รศ. ดร.ไพฑูรย์ รัชตะสาคร, อ.ที่ปรึกษาวิทยานิพนธ์ร่วม: รศ. ดร.มงคล สุขวัฒนา
 สันนิทธี, 61 หน้า.

สารเรืองแสงที่มีคุณสมบัติละลายน้ำได้เป็นสารที่มีความน่าสนใจสำหรับการวิเคราะห์สารเคมีหรือไอออนของโลหะที่ต้องการความไวและความแม่นยำสูง ดังนั้นในวิทยานิพนธ์ฉบับนี้จึงได้ออกแบบและสังเคราะห์สารอนุพันธ์ใหม่จำนวนสองชนิดขึ้นจากเฟอร์โรซีนที่มีสมบัติเป็นหมู่ให้อิเล็กตรอนที่ดีและ 1,8-แนพทาลิไมด์ซึ่งมีความพิเศษในสมบัติทางกายภาพเชิงแสง นอกจากนี้การเชื่อมต่อหมู่ไตรเอธิลีนไกลคอลในโครงสร้างยังช่วยเพิ่มความสามารถในการละลายน้ำ ซึ่งช่วยในการกระจายตัวของสารอนุพันธ์ในตัวกลางที่มีน้ำเป็นองค์ประกอบได้ดีมากขึ้น จากผลการศึกษาพบว่าสารอนุพันธ์ใหม่ทั้งสองชนิด มีความความยาวคลื่นการดูดกลืนแสงที่ยาวที่สุดอยู่ในช่วง 360-370 นาโนเมตร เมื่อสารอนุพันธ์นี้อยู่ในสถานะสารละลายผสมระหว่างน้ำและอะซิโตรไนไตรล์ จะให้ประสิทธิภาพการเรืองแสงฟลูออเรสเซนต์ที่ต่ำ เนื่องจากการมีหมู่เฟอร์โรซีนิลที่ทำหน้าที่เป็นตัวระงับสัญญาณการเรืองแสงฟลูออเรสเซนต์ของส่วน 1,8-แนพทาลิไมด์ ผ่านกระบวนการโฟโต้อินดิวิซอ์อิเล็กตรอนทรานส์เฟอร์ (PET) อย่างไรก็ตามหนึ่งในสองของสารอนุพันธ์ที่สังเคราะห์ขึ้น สามารถแสดงสมบัติการขยายสัญญาณการเรืองแสงในสถานะที่มีไอออน Au (III) หรือ Au (I) ในตัวกลางผสมของฟอสเฟตบัฟเฟอร์และอะซิโตรไนไตรล์ โดยปราศจากการรบกวนจากไอออนโลหะชนิดอื่น แม้ว่าจะมีความเข้มข้นสูงกว่าถึง 10 เท่าก็ตาม ในงานวิจัยนี้ได้ทำการศึกษาผลของอัตราส่วนของน้ำในตัวกลางผสมอะซิโตรไนไตรล์และเวลาการตอบสนองที่สัญญาณคงที่ ตลอดจนผลของ pH และสารลดแรงตึงผิว เพื่อให้ได้มาซึ่งสภาวะการตรวจวัดที่เหมาะสมที่สุด โดยภายใต้สภาวะดังกล่าวพบว่าสารเรืองแสงจะให้ค่าต่ำสุดที่สามารถตรวจวัดได้ (LOD) คือ 80 ppb

จุฬาลงกรณ์มหาวิทยาลัย
 CHULALONGKORN UNIVERSITY

ภาควิชา	เคมี	ลายมือชื่อนิสิต
สาขาวิชา	เคมี	ลายมือชื่อ อ.ที่ปรึกษาวิทยานิพนธ์หลัก
ปีการศึกษา	2556	ลายมือชื่อ อ.ที่ปรึกษาวิทยานิพนธ์ร่วม

5472044223 : MAJOR CHEMISTRY

KEYWORDS: FLUORESCENCE / FERROCENE / GOLD / NAPHTHALIMIDE / SENSOR

PONDCHANOK CHINAPANG: NEW FERROCENE-BASED FLUORESCENT CHEMOSENSOR. ADVISOR: ASSOC. PROF. PAITON RASHATASAKHON, Ph.D., CO-ADVISOR: ASSOC. PROF. MONGKOL SUKWATTANASINITT, Ph.D., 61 pp.

Two new compounds containing a ferrocene unit as a well-behaved electron-donor and a naphthalimide moiety as a strongly fluorescent transducer are designed and successfully synthesized. The incorporation of a hydrophilic triethyleneglycol unit can enhance the water-solubility and facilitate the dispersion of compounds in aqueous media. The incorporation of the ferrocene unit in both compounds results in molecules with low quantum efficiencies due to the photoinduced electron transfer (PET) from ferrocenyl to naphthalimide moiety. However, one of these compounds exhibits a selective fluorescent turn-on by the addition of Au (III) ion or Au (I) with low to negligible interference by 10-fold concentration of analytes to other metal ions in PBS buffer/acetonitrile. The effect of water content towards the response time and the effect of pH on sensitivity also the effect of surfactants of this sensor are investigated. Under optimum conditions, the detection limit for Au (III) ion was 80 ppb.



Department: Chemistry

Field of Study: Chemistry

Academic Year: 2013

Student's Signature

Advisor's Signature

Co-Advisor's Signature

ACKNOWLEDGEMENTS

The Master of Science program at Chulalongkorn University (CU) is a great program to provide opportunity for appealing-in-Scientific student to learn and get experiences in diversity knowledge with high skill colleagues. Faculty of Science as well as the department of Chemistry of CU is considered as one of the most innovative university for advanced research, full of professional staff and research facilities.

After I finished the Master program, I gain precious inspiration, knowledge, skills and laboratory experience. In addition, I have received a great chance in to exchange experience and new conceptual point of view with many graduated students and know-how staff. Gaining both theoretical knowledge and experience in research will also boost me up to become skillful graduated student. Thailand nowadays is still lack of specialists who have both knowledge and experience in science and technology. In my opinion, developing human resource capacity in science, technology and innovation is a good method to develop the country. Thus, Master program of Science at CU has been build up my dream to be a one who might help the country development.

I would like to thank Department of Chemistry, Faculty of Science and Chulalongkorn University for the research financial support and providing a great opportunity. I gratefully thank to Assoc. Prof. Paitoon Rashatasakhon and Assoc. Prof. Mongkol Sukwattanasinitt, my supervisor for giving me a chance to work under their supervision as well as their kindly supportive and suggestions. Special thanks are extended to Asst. prof. Sumrit Wacharasindhu and Dr. Anawat Achawakom for their generous cooperative and advantageous comments to my work. Appreciations to all MAPS group members and all Department of Chemistry members for their countless helpfulness and unforgettable friendships during I study in CU. Finally, I would like to express my gratitude to Assoc. prof. Shigeyuki Masaoka and Asst. prof. Mio Kondo at Institute for Molecular Science (IMS), Okazaki, Japan for their tenderhearted, honorable mind-setting and always believe in my ability. Special thanks are extended to Mr. Takahiro Itoh for the inspiration and let me understand that the quiet people have the loudest minds. Furthermore, I really appreciate all Masaoka group members for the valuable friendships and welcome me as a participant to their group in my doctoral program at IMS.

CONTENTS

	Page
THAI ABSTRACT	iv
ENGLISH ABSTRACT	v
ACKNOWLEDGEMENTS	vi
CONTENTS	vii
LIST OF TABLES	x
LIST OF FIGURES	xi
LIST OF SCHEMES	xiii
LIST OF ABBREVIATIONS	xiv
CHAPTER I INTRODUCTION.....	1
1.1 Introduction	1
1.2 Gold-detect fluorescent chemosensor	2
1.2.1 Gold: One of the most noble-metal	2
1.2.2 Recent progress on fluorescent chemosensors for gold ions	3
1.3 Fluorescent chemosensors.....	4
1.4 The principle of fluorescence spectroscopy	5
1.4.1 The Jablonski's diagram	6
1.4.2 Fluorescence spectra.....	7
1.4.3 Fluorescence transduction mechanism	8
1.4.3.1 Photo-induced Electron Transfer (PET).....	8
1.4.3.2 Internal Charge Transfer (ICT).....	9
1.4.4 Fluorescence properties.....	9
1.4.4.1 Quantum yield	9
1.4.4.2 The Stokes shift.....	10
1.5 Fluorescent sensors for gold detections	11
1.6 1,8-Naphthalimide as fluorophores.....	14
1.7 Ferrocenyl compounds as luminescent quencher and their applications.....	19
1.8 Objectives and scope of this research	21

	Page
CHAPTER II EXPERIMENTAL	22
2.1. Materials and instruments.....	22
2.2. Synthesis of 1 and 2.....	23
2.2.1 Synthesis of 4-bromo-N-(4'-hydroxyphenyl)-1,8-naphthalimide (3). 23	
2.2.2 Synthesis of 4-bromo-N-(4'-(2-(2-(2-methoxyethoxy)ethoxy)ethoxy)phenyl)-1,8-naphthalimide (4).....	23
2.2.3 Synthesis of fluorophore 1	24
2.2.4 Synthesis of 4-bromo-N-(4-iodo-phenyl)-1,8-naphthalimide (5) ...	25
2.2.5 Synthesis of 4-(2-(2-(2-methoxyethoxy)ethoxy)ethoxy)-N-(4'-iodophenyl)-1,8-naphthalimide (6)	25
2.2.6 Synthesis of fluorophore 2	26
2.4 Interference behaviors from other metal species on Au (III) signaling	27
2.5 Water content effect on reaction time and Au (III) signaling.....	27
2.6 pH effect on Au (III) signaling.....	28
2.7 Surfactant effect on Au (III) signaling.....	28
2.8 Limit of detection	28
2.9 Elucidation of sensing mechanism by ¹³ C-NMR spectroscopy	28
CHAPTER III RESULTS AND DISCUSSION.....	29
3.1. Synthesis and characterization of fluorophores.....	29
3.2. Photophysical properties of fluorophores.....	32
3.3. Selectivity screening of compound 1 and 2 toward various metal cations in aqueous media.....	36
3.4. Elucidation of the proposed sensing mechanism of compound 2 toward gold ions.....	38
3.5. Optimization of sensing conditions of compound 2 towards Au (III).....	40
3.6 Selectivity and sensitivity determination of compound 2 towards Au (III)	43
CHAPTER IV CONCLUSIONS.....	46
REFERENCES	47

VITA..... 61



จุฬาลงกรณ์มหาวิทยาลัย
CHULALONGKORN UNIVERSITY

LIST OF TABLES

	Page
Table 1.1 summarized precedent works related to fluorescent gold sensors available in the literature over the past five years.	11
Table 3.1 Photophysical properties of 1 and 2 in CH ₃ CN—H ₂ O (v:v = 1:1).....	32
Table 3.2. Effect of water content on fluorescence intensity of probe 2 towards Au (III) ion	40
Table 3.3. Fluorescence intensity of 2 (1 μM) when treated with 0.00 to 3.00 μM of Au (III) in mixture of PBS buffer solution (10 mM, pH 8.0) in CH ₃ CN (6/4, v/v).	45

LIST OF FIGURES

	Page
Figure 1.1 The important role of metallic elements.....	1
Figure 1.2 Some well-known gold-based drugs.	3
Figure 1.3 Main symptoms of gold toxicity on human body.	3
Figure 1.4 Schematic illustration of a chemical sensors.	4
Figure 1.5 Schematic illustration of two modes fluorescent chemosensor.....	5
Figure 1.6 Typical of some fluorescence substances.	6
Figure 1.7 Jablonski diagram.....	6
Figure 1.8 General diagram of the excitation and emission spectra for a fluorophore (left) and the intensity of the emitted light (Em1 and Em2) using different excitation wavelength.	7
Figure 1.9 Principle of the PET quenching mechanism	8
Figure 1.10 Principle of the ICT quenching mechanism.	9
Figure 1.11 Fluorophores with large (left) and small Stokes shifts (right).....	10
Figure 1.12 Structure of 1,8-naphthalimide.....	14
Figure 1.13 The general structure of synthesized 4-allyloxy-1,8-naphthalimide fluorescent brighteners for polystyrene copolymer (a-d).	14
Figure 1.14 Blue fluorescent polyacrylonitrile copolymers with 1,8-naphthalimides as fluorophore and their photophysical characteristics in DMF.....	15
Figure 1.15 Structure of 4- <i>N</i> -methyl piperazine-1,8-naphthalimide PPA dendrimer....	15
Figure 1.16 Binding mode of naphthalimide modified rhodamine B with Cu (II) in aqueous media (left: off-state; right: on-state).....	16
Figure 1.17 Confocal fluorescence images in HeLa cells. (a) Cells incubated with 20 μM chemosensor in PBS buffer for 30 min; (b) brightfield image of (a); (c) cells incubated with 1 μM of Cu(II), and then incubated with 20 μM of chemosensor for 30 min; (d) brightfield image of (c).	17
Figure 1.18 Proposed binding mechanism of 1,8-naphthalimide chemosensor with Hg (II) ion	17

Figure 1.19 Proposed mechanism of fluorescence quenching for the chemosensor upon addition of fluoride involved a disrupting intramolecular H-bond	18
Figure 1.20 Chemical structure of a Naph-BPEA fluorescent probe for sensing of Zn (II) ion.....	18
Figure 1.21 Confocal fluorescence images of HepG2 by 5 μ M of Naph-BPEA sensor. (a) bright field image of the stain cells; (b) fluorescence images of stain cells; (c) fluorescence image of (b) incubate with 5 μ M of ZnSO ₄ /pyrithione 20 min.; (d) fluorescence image of (c) treated by TPEN solution.....	19
Figure 1.22 The change of fluorescence quantum yield after the incorporating of ferrocenyl unit into 1,8-naphthalimide plateforms. (left: linked by saturated piperine spacer [56], right: linked by alkyne spacer).....	20
Figure 1.23 Fluorescence response of 9-AEF to HOCl	20
Figure 1.24 Structures of target compound 1 and 2	21
Figure 3.1 The comparison of ¹ H-NMR of compound 3, 4 and 1.	30
Figure 3.2 The comparison of ¹ H-NMR of compound 5, 6 and 2.	30
Figure 3.3 The physical appearance, mass spectroscopic analysis and ¹ H-NMR of compound 1.	31
Figure 3.4 The physical appearance, mass spectroscopic analysis and 1H-NMR of compound 2.....	31
Figure 3.5 Normalized absorption (solid line) and emission spectra (dashed line) of 1,8-naphthalimide 1 and 2 in CH ₃ CN—H ₂ O (1/1; v/v).....	32
Figure 3.6 Representative of π -conjugation at 4-position of 1 and 2.	33
Figure 3.7 Proposed charge separation in 2.....	33
Figure 3.8 Electron donating and withdrawing in 2.	34
Figure 3.9 Rational description of low fluorescence emission of 1 and 2	34
Figure 3.10 Fluorescence spectra of compound 1 (5 μ M, λ_{ex} 369 nm) in a mixture of CH ₃ CN-PBS buffer solution (pH 8.0, 10 mM, 1/1, v/v) upon addition of various metal ions (0.5 mM).	36

LIST OF SCHEMES

	Page
Scheme 1.1 Example of the catalytic mechanism of gold complex [9].....	2
Scheme 3.1 Synthesis of 1 and 2.....	29
Scheme 3.2 Proposed sensing mechanism of 2 towards Au (III) or Au (I) ion.....	38



LIST OF ABBREVIATIONS

Ar	aromatic
calcd	calculated
^{13}C NMR	carbon-13 nuclear magnetic resonance
CDCl_3	deuterated chloroform
CH_2Cl_2	Methylene chloride
CuI	Copper iodide
$\text{DMSO-}d_6$	deuterated dimethyl sulfoxide
DMSO	dimethylsulfoxide
d	doublet (NMR)
dd	doublet of doublet (NMR)
ESIMS	electrospray ionization mass spectrometry
EtOAc	Ethyl acetate
equiv	equivalent (s)
FT-IR	fourier transform infrared spectroscopy
g	gram (s)
^1H NMR	proton nuclear magnetic resonance
Hz	Hertz
HRMS	high resolution mass spectrum
h	hour (s)
IR	infrared
J	coupling constant
mg	milligram (s)
mL	milliliter (s)
mmol	millimole (s)
m.p.	Melting point
nm	Nanometer (s)
m/z	mass per charge

m	multiplet (NMR)
M.W.	molecular weight
M	molar
MHz	megaHertz
rt	room temperature
s	singlet (NMR)
THF	tetrahydrofuran
TLC	thin layer chromatography
UV	ultraviolet
δ	chemical shift
$^{\circ}\text{C}$	degree Celsius
μL	microliter (s)
μM	micromolar (s)
ϵ	Molar absorptivity
λ	Wavelength
Φ	quantum yield
%yield	percentage yield

CHAPTER I

INTRODUCTION

1.1 Introduction

Group \ Period	1	2	3	4	5	6	7	8	9	10	11	12	13	14	15	16	17	18
1	1 H																	2 He
2	3 Li	4 Be											5 B	6 C	7 N	8 O	9 F	10 Ne
3	11 Na	12 Mg											13 Al	14 Si	15 P	16 S	17 Cl	18 Ar
4	19 K	20 Ca	21 Sc	22 Ti	23 V	24 Cr	25 Mn	26 Fe	27 Co	28 Ni	29 Cu	30 Zn	31 Ga	32 Ge	33 As	34 Se	35 Br	36 Kr
5	37 Rb	38 Sr	39 Y	40 Zr	41 Nb	42 Mo	43 Tc	44 Ru	45 Rh	46 Pd	47 Ag	48 Cd	49 In	50 Sn	51 Sb	52 Te	53 I	54 Xe
6	55 Cs	56 Ba		72 Hf	73 Ta	74 W	75 Re	76 Os	77 Ir	78 Pt	79 Au	80 Hg	81 Tl	82 Pb	83 Bi	84 Po	85 At	86 Rn
7	87 Fr	88 Ra		104 Rf	105 Db	106 Sg	107 Bh	108 Hs	109 Mt	110 Ds	111 Rg	112 Uub	113 Uut	114 Uuq	115 Uup	116 Uuh	117 Uus	118 Uuo
	Lanthanides		57 La	58 Ce	59 Pr	60 Nd	61 Pm	62 Sm	63 Eu	64 Gd	65 Tb	66 Dy	67 Ho	68 Er	69 Tm	70 Yb	71 Lu	
	Actinides		89 Ac	90 Th	91 Pa	92 U	93 Np	94 Pu	95 Am	96 Cm	97 Bk	98 Cf	99 Es	100 Fm	101 Md	102 No	103 Lr	

Metallic elements are the major group of elements on earth [1], which can be classified into three principal categories, i.e. main group, transition and heavy metals. Almost all of the metal ions play important role in either biological system or environment. For example, Co (II), Ni (II), Cu (II), Zn (II), Fe (II) and Fe (III) are very important in biochemistry and are essential metal ions for human health. In contrary, some of these elements are toxic or act as harmful pollutants. Ions such as Cd (II), Hg (II) and Pb (II) are recognized as toxic metal ions that are very dangerous for human beings. For example, the abnormally high concentrations of mercury in the form of MeHgSMe in fish caused Minamata disaster in Japan in 1952. Thus, efficient methods concerning the qualitative and quantitative analysis of heavy metals need to be developed.

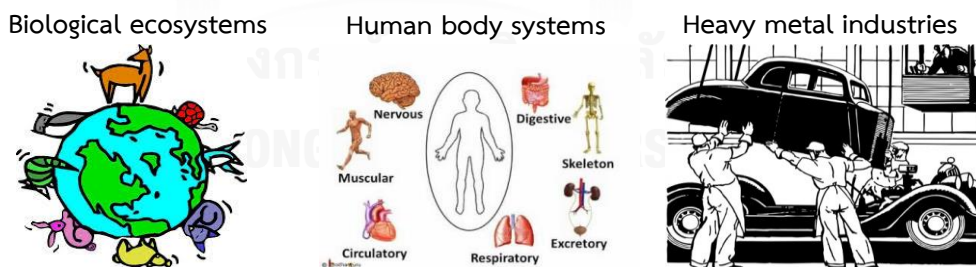
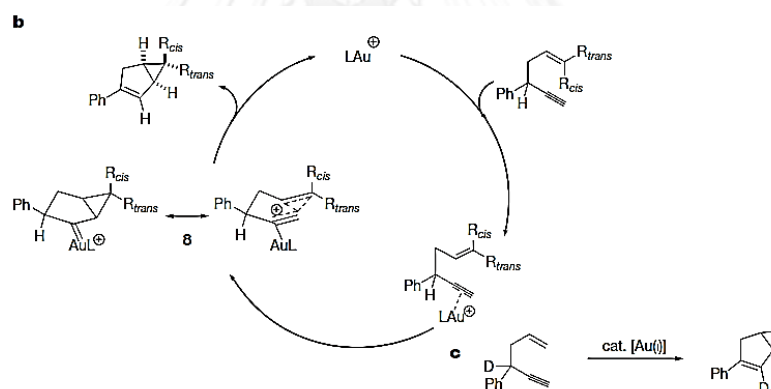


Figure 1.1 The important role of metallic elements.

1.2 Gold-detect fluorescent chemosensor

1.2.1 Gold: One of the most noble-metal

During the last decade, there has been much interests in gold species with respect to the unique chemical and physical properties of gold ions. Gold-related chemistry has triggered variable research. Gold species as gold-catalyst have been extensively in organic transformation owing to the “*alkynophilicity*” characteristic of gold ions, which have been known to activate carbon-carbon triple bond towards nucleophilic addition. The alkynophilic Lewis acidity of gold ions expands wide range potential applications in the area of gold-catalysed for organic transformations [2-8]. The gold catalysts are often in a form of cationic gold species **a** (Scheme 1.1) can coordinate to the alkyne to produce the gold-alkyne complex **b** containing a electrophilic site. Further reaction with intramolecular nucleophile then produces the structurally rearranged product.



Scheme 1.1 Example of the catalytic mechanism of gold complex [9].

In addition, gold nanoparticles (AuNPs), which possess distinct physical and chemical attributes make them excellent scaffolds for the fabrication of novel chemical and biological sensors [10, 11]. Several gold compounds have anti-inflammatory properties and used as pharmaceuticals. The well-known gold-based drugs such as Sanocrysin is valuable treatment of tuberculosis. Sologanol and Auronofin are also important in Rheumatic arthritis treatment and reducing viral reservoir of HIV [12].

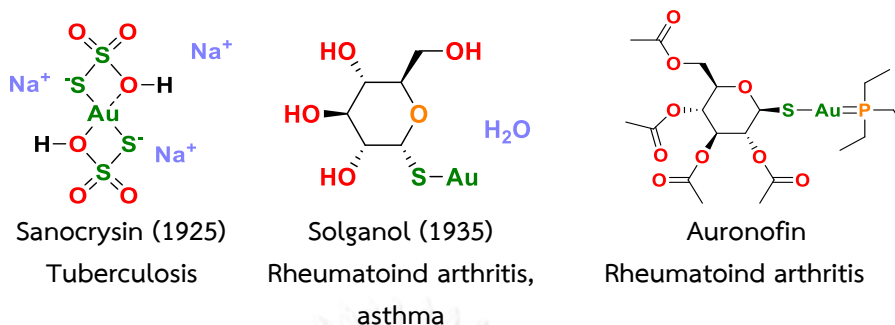


Figure 1.2 Some well-known gold-based drugs.

However, there are a few reports on toxicity of gold ions. Their soluble salts such as gold chloride are known to cause damage to the liver and kidneys because gold ions are able to bind strongly with DNA or biological tissue. In particular, some gold ion such as Au (III) are highly toxic to biological systems and cause undesirable DNA cleavage [13-18]. Therefore, it is highly urgent to develop gold ion probes to access the quantity in environmental and biological samples.

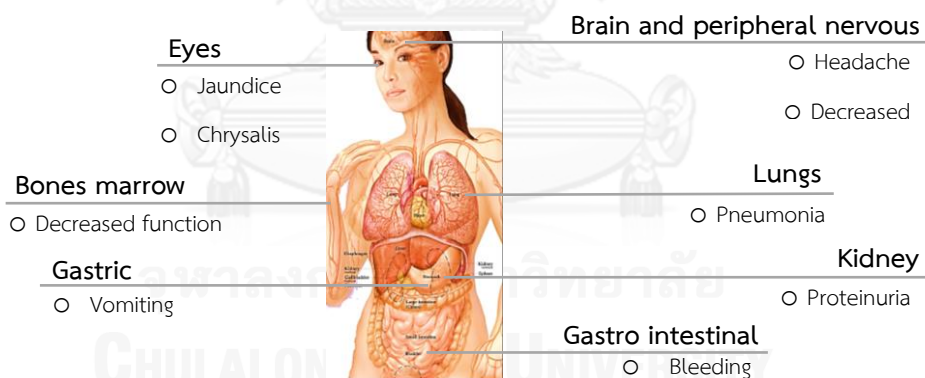


Figure 1.3 Main symptoms of gold toxicity on human body.

(http://www.prism.princeton.edu/PRISM_cleanroom/MSDS/Gold.pdf)

1.2.2 Recent progress on fluorescent chemosensors for gold ions

The trace analysis of metal ions in biological, clinical, or industrial samples are often carried out by many techniques. For example; spectroscopic methods (atomic absorption/emission with various atomizers), mass spectrometry (ICP-MS) and electrochemical technique (anodic stripping voltammetry). By the way, most of these

analysis methods have several drawbacks, for example, expensive installation and complicated maintenance of instruments, requirement of skilled specialists or operators, demands of sample pre-treatment and time-consuming.

On the other hand, the fluorescence method is more convenient in terms of simple operation, cost effectiveness, rapid and real-time operation, and high sensitivity. These could provide a simple detection method for determination of trace elements outside the laboratory. Therefore, this research focuses on development of new fluorescent chemosensor for detection of metal ions.

1.3 Fluorescent chemosensors

As defined by the Oxford English Dictionary, sensors are devices that detect or measure a physical property and record, indicate or otherwise respond to a certain analyte. A chemical sensor is a device that qualitatively or quantitatively detects the presence of specific chemical substances using a specific chemical interaction or reaction [19]. Chemosensors based on fluorescence signal changes are commonly referred to as fluorescent chemosensors [20] which are gaining increased attention due to their high sensitivity and specificity.

Generally, a fluorescent sensor device contains two main components: a receptor (binding site) and a signal transducer (signaling unit) linked by a spacer. (**Figure 1.4**). In most cases, the spacer is not responsible for signal transduction. The receptor is a fragment designed to respond to a specific stimulus or locate a specific target substance (the analyte). A powerful sensor must exhibit a selective receptor-to-analyte complex formation depending on the size, shape, binding energy, or interaction of the receptor and analyte.

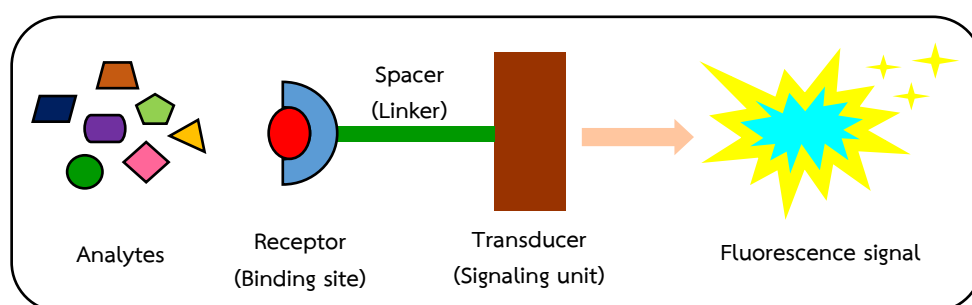


Figure 1.4 Schematic illustration of a chemical sensors.

Signal transduction is the process through which an interaction of receptor with analyte yields a measurable form of energy change and is converted to a signal change that can be read and quantified. The read-out domain is the part responsible for reporting either the binding or reactivity event [21]. It is usually measured as a change in fluorescence signal intensity, intensity decay lifetime or shift of emission wavelength.

Based on their changes in fluorescent intensities, fluorescent sensors can be categorized into two groups. The “turn-on” sensors are those which exhibit stronger intensity under the presence of analyte. Sensors which show opposite changes in fluorescent signal would be called “turn-off” sensors (**Figure 1.5**).

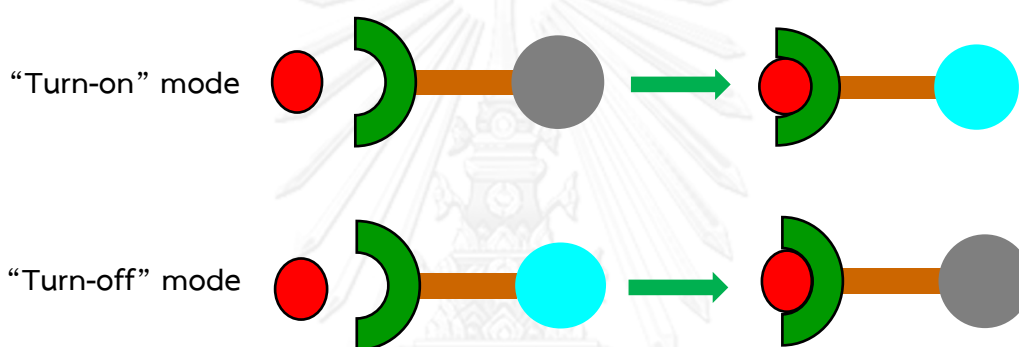


Figure 1.5 Schematic illustration of two modes fluorescent chemosensor.

1.4 The principle of fluorescence spectroscopy

Fluorescence is the emission of photons following relaxation from an excited electronic state to the ground state [22]. Basically, fluorescence occurs in certain conjugated molecules (generally polyaromatic hydrocarbons or heterocycles) called fluorophores or fluorescent dyes. To describe the process occur between absorption and emission of light, Jablonski's diagram is used to explain the fluorescence process that occur in fluorescence chemosensors.

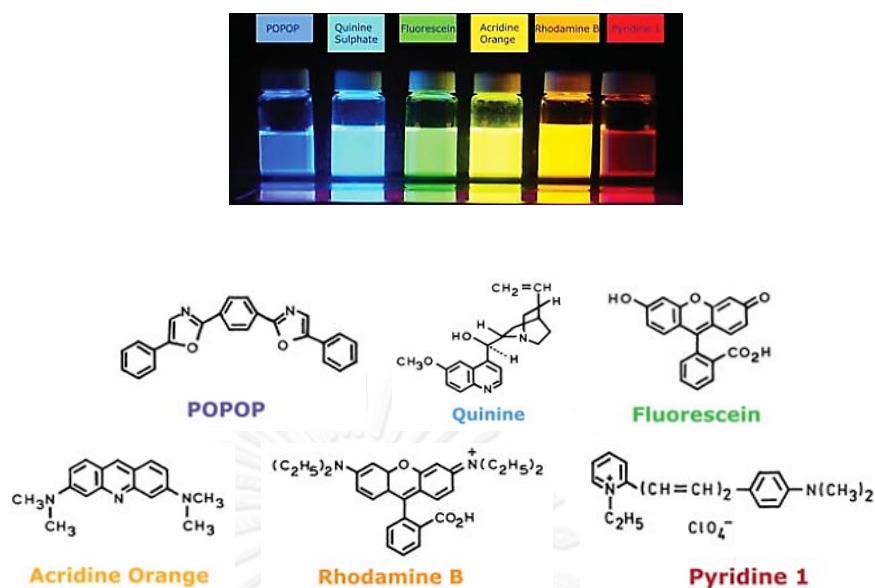


Figure 1.6 Typical of some fluorescence substances [22].

1.4.1 The Jablonski's diagram

The processes that occur between the absorption and emission of light which is responsible for the fluorescence is illustrated by the Jablonski's diagram (Figure 1.7). In this diagram, the singlet ground, first, and second electronic states are depicted by S_0 , S_1 , and S_2 , respectively. At each of these electronic energy levels the fluorophores can exist in a number of vibrational energy levels. The transitions between states are depicted as vertical lines to illustrate the instantaneous nature of light absorption. Transitions occur in about 10^{-15} s, a time too short for significant displacement of nuclei [22].

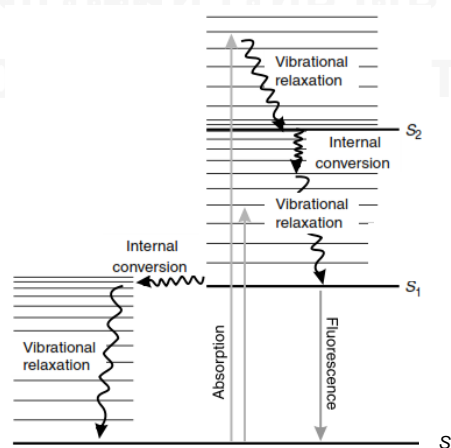


Figure 1.7 Jablonski diagram.

Following light absorption, several processes can occur. A fluorophore is usually excited to some higher vibrational level of either S_1 or S_2 . With a few rare exceptions, molecules in higher excited state phases rapidly relax to the lowest vibrational level of S_1 . This process is called internal conversion and generally occurs within 10^{-12} s or less. Since fluorescence lifetimes are typically near 10^{-8} s, internal conversion is generally complete prior to emission. Hence, fluorescence emission generally results from a thermally equilibrated excited state, that is, the lowest energy vibrational state of S_1 .

1.4.2 Fluorescence spectra

Fluorescence data are generally presented as emission spectra which are plots of the fluorescence intensity versus either wavelength (nm) or wavenumber (cm^{-1}). In general, the highest emission intensity can be obtained when the compound is irradiated by light of maximum absorption wavelength. The excitation using light at other wavelengths will lead to an emission band at the same position, albeit in lower intensity (**Figure 1.8**). It is also important to note that emission spectra vary widely and are dependent upon the chemical structure of the fluorophore and the solvent in which it is dissolved [22].

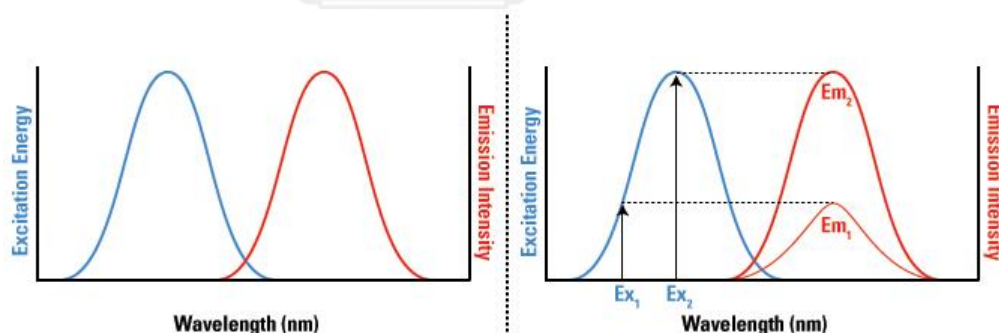


Figure 1.8 General diagram of the excitation and emission spectra for a fluorophore (left) and the intensity of the emitted light (Em_1 and Em_2) using different excitation wavelength.

1.4.3 Fluorescence transduction mechanism

An important feature of the fluorescent chemosensors is that signal transduction of analyte binding event into the readout signal can happen in a very short time and without any other assistance. Currently, fluorescent sensors can be designed on basis of various binding mechanism between analyte and receptor unit involves photophysical such as photo-induced electron transfer (PET), photo-induced charge transfer (PCT), internal charge transfer (ICT), fluorescence resonance energy transfer (FRET) and excimer/excimer formation or extinction. These mechanisms make real-time and real-space detection of the analyte distribution [22]. Thus, it is not surprising that in the last decade the development of fluorescent sensors for metal ions on various principles has become a very active area of research [20]. Great effort has recently been devoted to the design and construction of molecular sensory system for a broad range of environmental and biological analyses.

1.4.3.1 Photo-induced Electron Transfer (PET)

When the fluorophore is excited, the electron in the highest occupied molecular orbital (HOMO) is promoted to the lowest unoccupied molecular orbital (LUMO). This enables the electron transfer from the HOMO of the donor (belonging of the free cation receptor) to that of the fluorophore (Figure 1.9, left) resulting in low or undetectable emission. When this system (sensors) is in the presence of the analyte, the energy of bound receptor will be lower, thus the PET can be disrupted and the system can emit upon excitation (Figure 1.9, right).

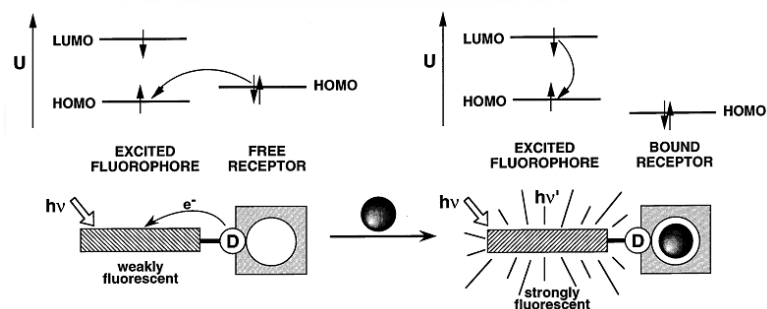


Figure 1.9 Principle of the PET quenching mechanism [22].

1.4.3.2 Internal Charge Transfer (ICT)

If the fluorophore possesses both electron-donating and electron-withdrawing groups, its structure at excited states may be those with a charge separation. When these structures are relatively stable, the molecule may be well-populated in the more stable electronic state compared to the locally excited state, as known as the ICT state. This process gives rise to the emission at a longer wavelength or lower intensity due to significant geometry changes (Figure 1.10).

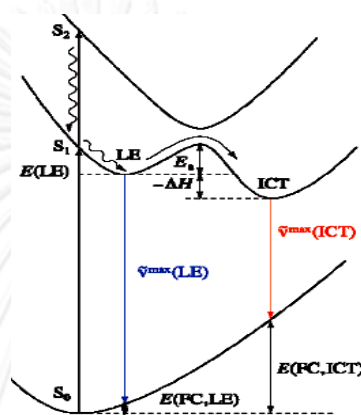


Figure 1.10 Principle of the ICT quenching mechanism [22].

1.4.4 Fluorescence properties

1.4.4.1 Quantum yield

For any fluorescence compounds, the ability to give the intense signal could be estimated from the magnitude of a quantum yield the fraction of the number of quanta absorbed by a molecule that are emitted as fluorescence is termed the fluorescence quantum yield. In the other word, the quantum yield is value that relates to their emission efficiency.

The most widely used method of determining quantum yield is by the relative method. In this procedure, the quantum yields are measured between the absorbance at the maximum absorption wavelength and the sum of all fluorescent intensity at the same absorbance. Then the slope or gradient from plot of sum fluorescence intensity and absorbance of compound was calculated following the equation [23], where Φ is the quantum yield, *Grad* is the gradient from the plot of integrated fluorescence intensity vs absorbance and η is the refractive index of the solvent. Subscript STD and x refer to standard and tested compound, respectively.

$$\Phi_{X=ST} \left(\frac{Grad_X}{Grad_{ST}} \right) \left(\frac{\eta_X^2}{\eta_{ST}^2} \right)$$

1.4.4.2 The Stokes shift

In general, the energy of the emission is typically less than that of absorption. Fluorescence typically occurs at lower energies or longer wavelengths. When a photon of energy is emitted, returning the fluorophore to its ground state S_0 . Due to energy dissipation during the excited-state lifetime, the energy of this photon is lower, and therefore of longer wavelength, than the excitation photon. The difference in energy or wavelength represented by Stokes shift ($h\nu_{EX} - h\nu_{EM}$) (Figure 1.11).

The Stokes Shift is a key aspect in the detection of the emitted fluorescence in biological applications and also a distinct characteristic of each fluorophore. For example, the detection of emitted fluorescence can be difficult to distinguish from the excitation light when using fluorophores with very small Stokes shifts (left), because the excitation and emission wavelengths greatly overlap. Conversely, fluorophores with large Stokes shifts (right) are easy to distinguish because of the large separation between the excitation and emission wavelengths. The Stokes shift is fundamental to the sensitivity of fluorescence techniques because it allows emission photons to be detected against a low background, isolated from excitation photons. In contrast, absorption spectrophotometry requires measurement of transmitted light relative to high incident light levels at the same wavelength [22].

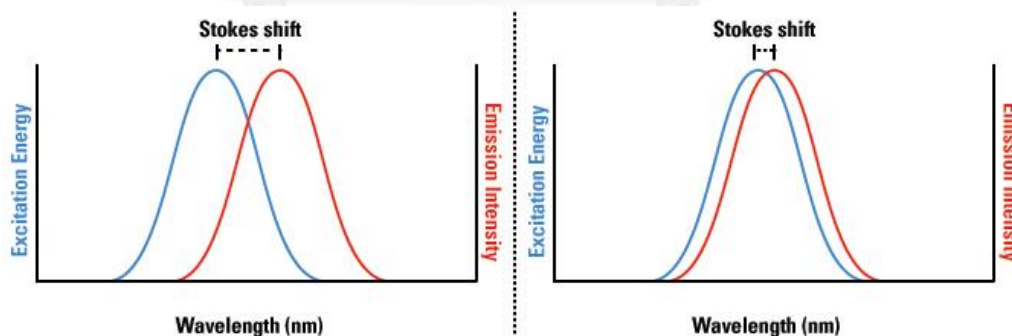
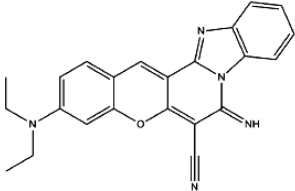


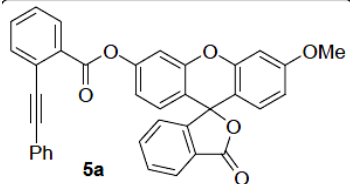
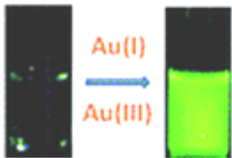



Figure 1.11 Fluorophores with large (left) and small Stokes shifts (right) [22].

1.5 Fluorescent sensors for gold detections

Table 1.1 summarized precedent works related to fluorescent gold sensors available in the literature over the past five years.

<p>Compound [24]:</p>  <p>Photophysical properties:</p> <p>$\lambda_{\text{abs}} = 552 \text{ nm}$</p> <p>$\lambda_{\text{exc}} = 390 \text{ nm}$</p> <p>$\Phi = 0.22$</p>	<p>Conditions: MeCN-HEPES buffer (10 mmol L⁻¹, pH 7.4, 1:1 v/v)</p> <p>Detection mode: Turn-off</p> <p>Reaction time: 30 sec.</p> <p>LOD: 1.23 $\mu\text{mol L}^{-1}$</p> <p>Fluorescence change:</p>  <p>Visible color change:</p> 
<p>Compound [25]:</p>  <p>Photophysical properties:</p> <p>$\lambda_{\text{abs}} = 313 \text{ to } 452 \text{ nm}$</p> <p>$\lambda_{\text{ems}} = 515 \text{ nm}$</p>	<p>Conditions: MeCN-PBS buffer (10 mmol L⁻¹, pH 7.4, 1:1 v/v)</p> <p>Ion detections: Au(I) and Au(III)</p> <p>Detection mode: Turn-on</p> <p>Reaction time: Abs, after 40 min. Ems, after 30 min. (sat. after 3h.)</p> <p>LOD: 5-80 $\mu\text{mol L}^{-1}$</p> <p>Fluorescence change:</p>  <p>Visible color change:</p> 

Compound [26]:



Photophysical properties:

$$\lambda_{\text{abs}} = 366, 520 \text{ nm}$$

$$\lambda_{\text{ems}} = 511 \text{ nm}$$

Conditions: MeCN-Acetate buffer

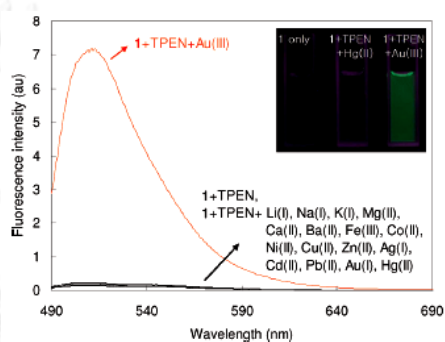
$$(10 \text{ mmol L}^{-1}, \text{pH } 4.7, 1:1 \text{ v/v})$$

Detection mode: turn on

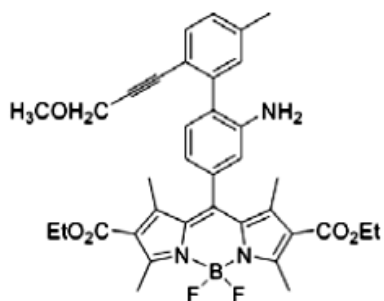
Reaction time: 1 min.

LOD: $0.11 \mu\text{mol L}^{-1}$

Fluorescence and spectral change:



Compound [27]:



Photophysical property:

$$\lambda_{\text{ems}} = 511 \text{ nm}$$

Conditions: EtOH-PBS buffer

$$(10 \text{ mmol L}^{-1}, \text{pH } 7.4, 1:1 \text{ v/v})$$

Ion detections: Au(I) and Au(III)

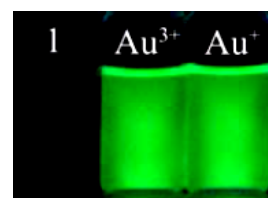
Detection mode: Turn-on

Reaction time: measured after 30 min then saturated after 60 min.

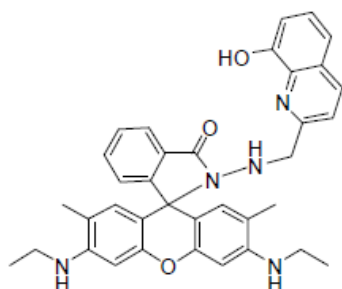
LOD: 320 nmol L^{-1} , 63 ppb

Metal ion interferences: Hg^{2+} and Pd^{2+}

Fluorescence change:



Compound [28]:



Photophysical properties:

$$\lambda_{\text{abs}} = 543 \text{ nm}$$

$$\lambda_{\text{ems}} = 556 \text{ nm}$$

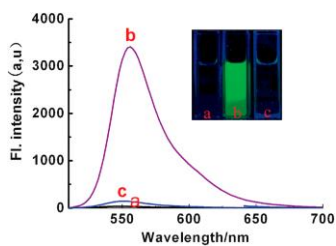
Conditions: H₂O-EtOH (7:3 v/v) pH: 5.5 – 8.0

Ion detection: Au(III)

Detection mode: Reversible turn-on

LOD: 48 nmol L⁻¹

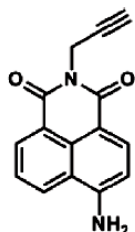
Fluorescence and spectral change:



Visible color changes:



Compound [29]:



Photophysical properties:

$$\lambda_{\text{ems}} = 543 \text{ nm}$$

in H₂O (0.05% DMSO v/v)

$$= 509 \text{ nm}$$

in CH₃OH (5% H₂O v/v)

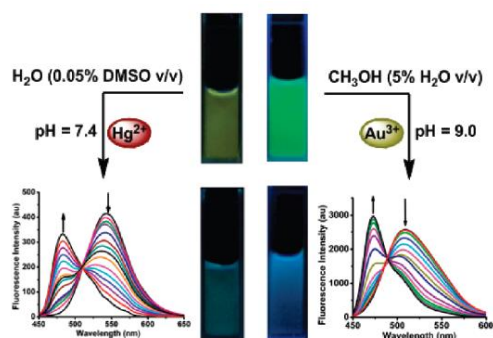
Conditions: MeOH-H₂O (95:5 v/v, pH 9.0)

Ion detections: Hg(II) or Au(III)

Detection mode: Fluorescence color change
(Blue shift)

LOD: 100 μmol L⁻¹

Fluorescent spectral change:



1.6 1,8-Naphthalimide as fluorophores

During the past few years, there has been upsurge in the number of reports on the photophysics and applications on 1,8-naphthalimide-based compound [30-35]. 1,8-Naphthalimide is obtained from reaction of 1,8-naphthalic anhydride with various amines which can be decorated on their applications. Due to their advantageous optical properties, such as strong absorption and emission in visible region, high fluorescence quantum yields, large Stokes shift, high photo stability and insensitive to pH. These remarkable photophysical properties are because of the ICT process that is caused by “push-pull” substituent pairs (electron donor-acceptor pairs) between electron donor at 4-position and electron acceptor at *N*-imide [36].

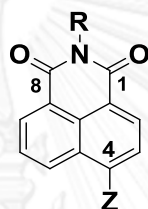


Figure 1.12 Structure of 1,8-naphthalimide.

In this research, 1,8-naphthalimide has chosen as fluorophore unit with excellent stability and high fluorescence quantum yield. Some of them have been used as fluorescent brightening agents for polymer. In 2001, Vladimir Bojinov and Ivo Grabchev [37] reported a new method for synthesis of four (a-d) 4-allyloxy-1,8-naphthalimide fluorescent brighteners. All product are colorless and displayed intense blue fluorescence in toluene with quantum yields of 0.43, 0.47, 0.48 and 0.51, respectively. Then, resulted polystyrene copolymer with 4-allyloxy-1,8-naphthalimide derivatives could emit intensive blue fluorescence emission.

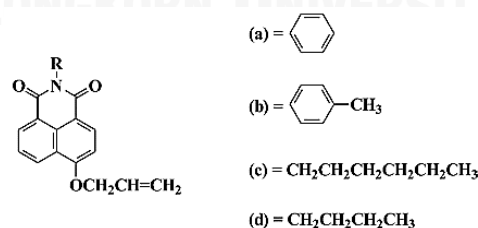
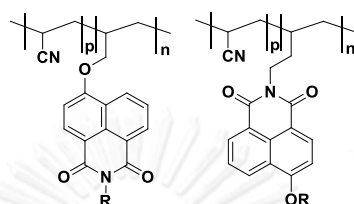


Figure 1.13 The general structure of synthesized 4-allyloxy-1,8-naphthalimide fluorescent brighteners for polystyrene copolymer (a-d) [37].

And also, as the blue emissive polymers have been established by Vladimir Bojinov in 2002 [38]. Monomeric 4-alkoxy-1,8-naphthalimide derivatives have been investigated as blue emitting fluorophore. In this study, the copolymerization of acrylonitrile with 4-alkoxy-1,8-naphthalimides resulted high photostability and intensive blue excellent fluorescence quantum yield emission in range 0.49-0.75.



Where R = CH₃ (Ia), C₂H₅ (Ib), C₃H₈ (Ic)

R = C₄H₉ (IIa), C₆H₁₃ (IIb), C₆H₅ (IIc), p-C₆H₅-CH₃ (IId)

Figure 1.14 Blue fluorescent polyacrylonitrile copolymers with 1,8-naphthalimides as fluorophore and their photophysical characteristics in DMF [38].

In 2011, Ivo Grabchev et al. prepared a new green fluorescent poly(popyleneamine) dendrimers second generation, having eight 4-N-methylpiperazine-1,8-naphthalimide signaling units in its dendrimers periphery. To investigated in THF, this new dendrimers shown good fluorescent emission with quantum yield determined to be 0.69 [39].

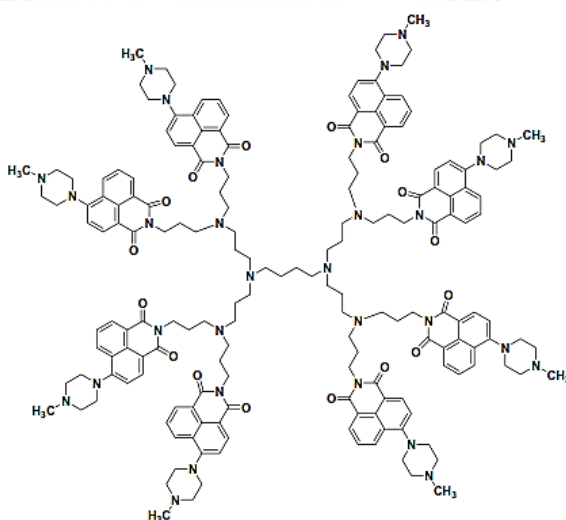


Figure 1.15 Structure of 4-N-methyl piperazine-1,8-naphthalimide PPA dendrimer [39].

Consequently, the 1,8-naphthalimide structure has been extensively used within the ion recognition and sensing of cations or anions, as a fluorescent chemosensor with strongly absorbing and emitting characteristic. Interestingly, some of them could be also used as fluorescent markers in biological systems. The examples presented herein has variable receptor moiety on naphthalimide fluorophore, commonly, 4-position or 1,8-imide site. Thus, up until now, there have been enormous researches on an ion recognition and sensing system involving the naphthalimide fluorophore.

In 2011, Lingxin Chen et al. have been reported a novel “off-on” fluorescent chemosensor of naphthalimide modified rhodamine B, based on the equilibrium between spirolactam (non-fluorescence) and the ring-opened amide (fluorescence). The chemosensor shown Cu(II)-selectivity over various metal ions and anions in neutral ethanol-HEPES solution [40].

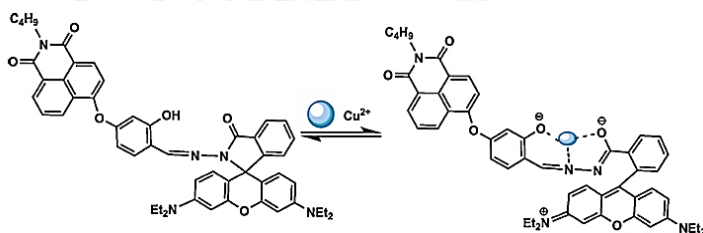


Figure 1.16 Binding mode of naphthalimide modified rhodamine B with Cu (II) in aqueous media (left: off-state; right: on-state) [40].

And also, in this report has been demonstrated the practical applicability of the visualizing fluorescence image of Cu (II) ions in HeLa cell samples. Their fluorescence images were recorded at 37°C before and after the addition of Cu (II) ion 30 min.

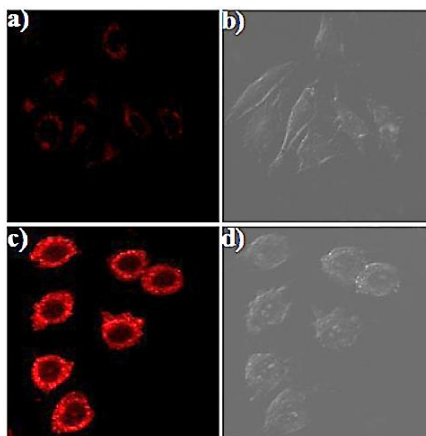


Figure 1.17 Confocal fluorescence images in HeLa cells [40]. (a) Cells incubated with 20 μM chemosensor in PBS buffer for 30 min; (b) brightfield image of (a); (c) cells incubated with 1 μM of Cu(II), and then incubated with 20 μM of chemosensor for 30 min; (d) brightfield image of (c).

In the same year, Hui Xu et al. have been successfully designed and synthesized a new simple water-soluble “turn-on” fluorescent chemosensor containing two acetic carboxylic moieties. The chemosensor exhibits high selectivity and selectivity with fluorescent enhancement on Hg (II) in water *via* inclusion complex over other heavy and transition metal (HTM) ions which are considered as severe environmental pollutants [41].

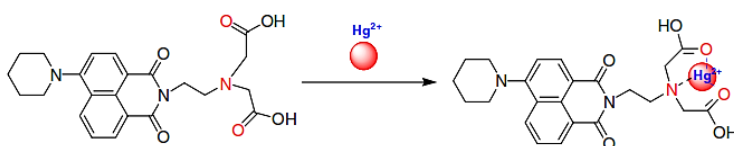


Figure 1.18 Proposed binding mechanism of 1,8-naphthalimide chemosensor with Hg (II) ion [41].

Haishi Cao et al. [42] have reported a new *N*-imidazole functionalized naphthalimide for sensing of F^- , a design that displays strong fluorescence due to coplanar geometry formed by intramolecular H-bond between imidazole and naphthalimide moieties. The addition of F^- resulted decreasing in the fluorescence emission at 442 nm with 94% quenching, due to the disruption of the H-bond, which is referred to “fluoride-triggered disruption”. Consequently causes fluorescence signal quenching. This quenching strategy provides a powerful “on-off” signal change for fluorescence sensing on the basis of 1,8-naphthalimide.

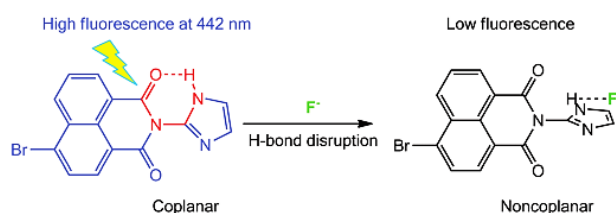


Figure 1.19 Proposed mechanism of fluorescence quenching for the chemosensor upon addition of fluoride involved a disrupting intramolecular H-bond [42].

Zijian Guo et al. recently developed a new fluorescent sensor [43], Naph-BPEA, shows a specific turn-on response to $Zn(II)$ ion in the green emission region. The titration profile based on emission at 540 nm and that based on absorption profile at 400 nm suggest a 1:1 of $Zn(II)$ binding stoichiometry to a sensor probe. The quantum yield of $Zn(II)$ -Naph-BPEA complex was determined to be 0.19. In addition, the detection limit of this sensor was calculated to be 57 nM. Thus, this sensor might be a powerful candidate as fluorescent imaging agent for intracellular $Zn(II)$ ion. Consequently, this sensor is able to $Zn(II)$ ion imaging in HepG2 cells were demonstrated.

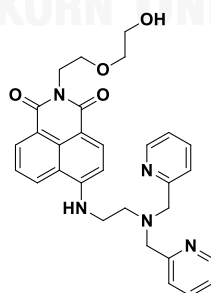


Figure 1.20 Chemical structure of a Naph-BPEA fluorescent probe for sensing of $Zn(II)$ ion [43].

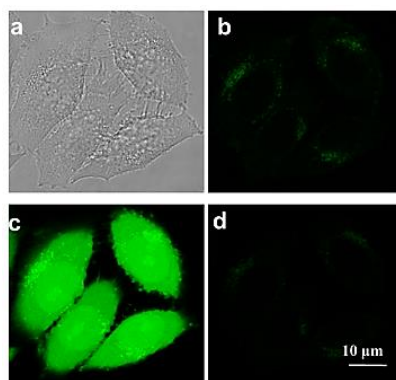


Figure 1.21 Confocal fluorescence images of HepG2 by 5 μM of Naph-BPEA sensor. (a) bright field image of the stain cells; (b) fluorescence images of stain cells; (c) fluorescence image of (b) incubate with 5 μM of ZnSO_4 /pyrithione 20 min.; (d) fluorescence image of (c) treated by TPEN solution [43].

1.7 Ferrocenyl compounds as luminescent quencher and their applications

Ferrocene and ferrocenyl derivatives fulfill many of broad criteria for development of molecular materials for specific technological applications. As far as we know, their chemistry are well-known and often appreciated for their outstanding stability. For example, ferrocene has high photo-stability under visible irradiation, good electron donating moieties, excellent redox reversible. Ferrocene has been widely used as luminescence excited state quenchers and may undergo chemical modification to a number of various ferrocene-based compounds. Their chemistry are well known and considerable interest in various areas, like asymmetric catalysis [44, 45], artificial photosynthesis [46-50] and electrochemistry [51-53].

Furthermore, ferrocenyl derivatives are well known as efficient fluorescence quenchers which led to numerous applications in the areas of analytical chemistry, molecular organized systems, and biology [52, 54, 55]. On the other hand, literature reports indicate that ferrocene has proved to be a simple building block for the preparation of derivatives which can be explored for the quenching state of analytes.

Owing to its remarkable photophysical properties, In 2002, Jiaan Gan et al. [56] has been reported a series of ferrocene derivatives containing 4-amino-1,8-naphthalimide linked on 4-position of naphthalimide ring through $-\text{CH}=\text{N}-$ spacer. After incorporated of ferrocene into the naphthalimide, the significantly decrease of fluorescence quantum yield was found. Thus, their electrochemical and photophysical

resulted interaction between ferrocene and naphthalimide moieties was appended *via* PET quenching mechanism.

Later in 2010, Tei Tagg et al. [57] prepared and characterized dyads containing ferrocene donor and naphthalimide acceptor unit, separated by alkyne bond spacer. It has been found that the attachment of ferrocenyl substituent in to 4-position of 1,8-naphthalimide which it caused dramatically decrease of fluorescence emission efficiency.

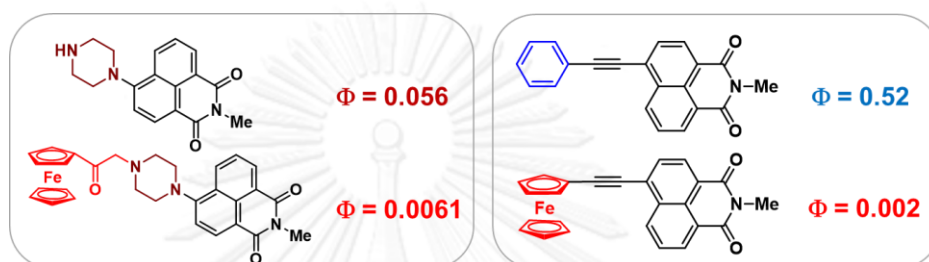


Figure 1.22 The change of fluorescence quantum yield after the incorporating of ferrocenyl unit into 1,8-naphthalimide platforms. (left: linked by saturated piperine spacer [56], right: linked by alkyne spacer [57])

In the same year, Huimin Ma et al. [58] has been prepared and characterized a highly specific ferrocene-based fluorescent probe, (9-anthryl)ethynylferrocene, 9-AEF for HOCl sensing. The designed strategy is based-on the strong quenching effect of good electron-donor ferrocene on anthracene fluorescence *via* an ICT quenching process. Then, in the presence of HOCl, the fluorescence was enhancement, the quantum yield from less than 0.001 to be 0.12. The limit of detection was determined to be 0.3 μM .

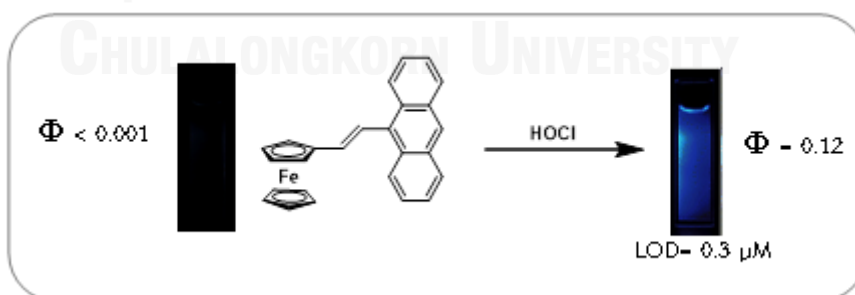


Figure 1.23 Fluorescence response of 9-AEF to HOCl [58].

1.8 Objectives and scope of this research

From the information described above, it is our intention to design and synthesize new 1,8-naphthalimide derivatives containing a ferrocene moiety. These new materials should exhibit relatively low emission efficiency due to the PET process between the naphthalimide and ferrocene. Analytes which can prevent this quenching mechanism could therefore cause an enhancement or restoration of the fluorescence signal. After that, the photophysical properties of these compounds are investigated. The application of these new target compounds as metal ion sensors in aqueous media and their optimal measurement conditions will also be explored. The structures of target compounds are shown in **Figure 1.24**.

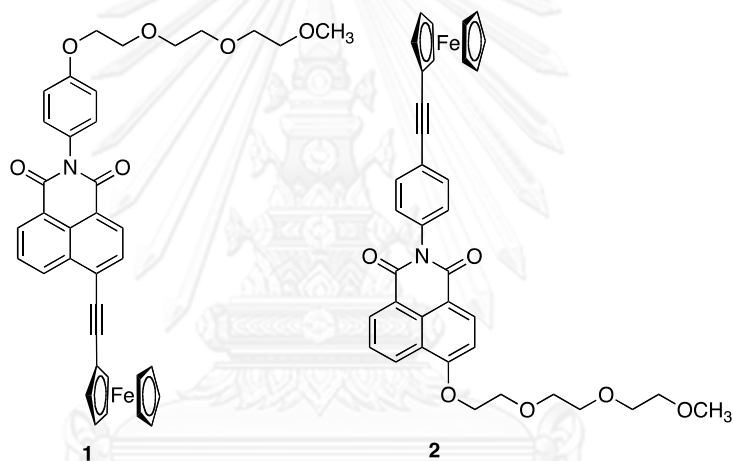


Figure 1.24 Structures of target compound 1 and 2.

CHAPTER II

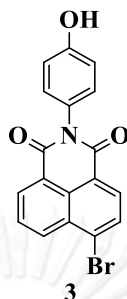
EXPERIMENTAL

2.1. Materials and instruments

4-Bromo-1,8-Naphthalic anhydride, 4-methoxy aniline, 4-iodo aniline, triethylene glycol monomethyl ether, sodium hydride, 4Å molecular sieve, tetrakis(triphenylphosphine)palladium and tris(dibenzylideneacetone)dipalladium, were purchased from Sigma-Aldrich (USA) and used without purification. Potassium carbonate, 1H-imidazole, copper iodide, triphenyl phosphine were purchased from Fluka (Switzerland) and used without purification. Ethynyl ferrocene was purchased from Chemieliva (China) and used without purification. All chemicals were reagent grades. Spectroscopic grade acetonitrile for fluorescence measurement was purchased from Fluka (Switzerland). All organic solvents for reaction work up and chromatography were commercial grades, which were distilled prior to use. HAuCl_4 and AuCl were purchased from Sigma-Aldrich (USA). Other inorganic salts were in perchlorate, acetate, chloride or nitrate form. Thin layer chromatography (TLC) was performed on aluminum sheets pre-coated with silica gel (Merck Kieselgel 60 F254) (Merck KGaA, Darmstadt, Germany). Column chromatography was performed on silica gel (Merck Kieselgel 60G) (Merck KGaA, Darmstadt, Germany). All ^1H - and ^{13}C -NMR spectra were obtained on a Varian Mercury NMR spectrometer, which operated at 400 MHz for ^1H and 100 MHz for ^{13}C nuclei (Varian Company, CA, USA). Absorption spectra were measured by a Varian Cary 50 UV-Vis spectrophotometer. Fluorescence spectra were obtained from a Varian Cary Eclipse spectrofluorometer.

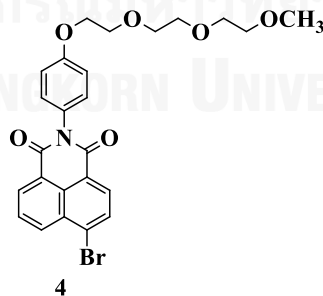
2.2. Synthesis of 1 and 2

2.2.1 Synthesis of 4-bromo-N-(4'-hydroxyphenyl)-1,8-naphthalimide (3).



This compound was synthesized by a modified method described in the literature [35]. A mixture of commercially available 4-bromo-1,8-naphthalic anhydride (1.0 g, 3.61 mmol), 10 mL of glacial acetic acid, and 4-hydroxyaniline (0.79 g, 7.22 mmol) was refluxed overnight. After the reaction was cooled to room temperature, it was poured into ice water and the dark purple precipitate was filtered and washed with water. The crude product was purified by silica gel column chromatography using ethyl acetate/hexane (1:4) as eluent. The product (**3**) was obtained as an off-white powder in 63% yield. ¹H NMR (400 MHz, CDCl₃, δ ppm): 8.64 (1H, d, *J* = 8.0 Hz), 8.57 (1H, d, *J* = 8.0 Hz), 8.39 (1H, d, *J* = 8.0 Hz), 8.01 (1H, d, *J* = 8.0 Hz), 7.80 (1H, t, *J* = 8.0 Hz), 7.15 (2H, d, *J* = 8.8 Hz), 7.00 (2H, d, *J* = 8.8 Hz).

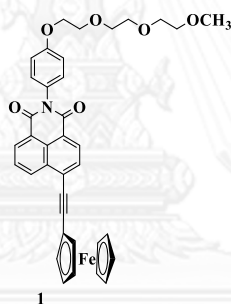
2.2.2 Synthesis of 4-bromo-N-(4'-(2-(2-(2-methoxyethoxy)ethoxy)ethoxy)ethoxy)phenyl)-1,8-naphthalimide (4).



A mixture of **3** (0.25 g, 0.68 mmol), K₂CO₃ (0.19 g, 1.36 mmol) and TBAF (0.04 g, 0.14 mmol) in CH₃CN (7 mL) was stirred at room temperature for 1 h. Then, 1-iodo-2-(2-(2-methoxyethoxy)ethoxy)ethane (0.35 g, 1.36 mmol) [59] was added in one portion and the reaction was heated under reflux conditions and monitored by TLC. After the

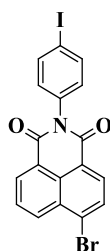
reaction completed, the mixture was concentrated under reduced pressure. The residue was re-dissolved in CH_2Cl_2 and the solution was sequentially washed with water, 5% HCl, and brine. After drying of the organic solution over anhydrous MgSO_4 and evaporation of the solvent, the residue was purified by silica gel chromatography using gradient eluents from EtOAc/hexane (4:1) to pure EtOAc to afford **4** as an off-white solid in 46% yield. ^1H NMR (400 MHz, CDCl_3 , δ ppm): 8.68 (1H, d, $J = 7.3$ Hz), 8.60 (4H, d, $J = 8.5$ Hz), 8.43 (1H, d, $J = 7.8$ Hz), 8.05 (1H, d, $J = 7.9$ Hz), 7.86 (1H, t), 7.14 (2H, d, $J = 8.6$ Hz), 7.06 (2H, d, $J = 8.6$ Hz), 4.19 (2H, t), 3.89 (2H, t), 3.79 – 3.73 (2H, m), 3.73 – 3.64 (4H, m), 3.60 – 3.52 (2H, m), 3.39 (3H, s). ^{13}C NMR (100 MHz, CDCl_3 , δ ppm): 164.1, 164.0, 159.0, 130.9, 133.6, 132.5, 131.7, 131.3, 130.7, 129.4, 129.4, 128.3, 127.8, 123.4, 122.6, 115.5, 72.1, 71.1, 70.8, 70.7, 69.8, 67.8, 59.1. MS (MALDI-TOF) Calcd for $\text{C}_{25}\text{H}_{24}\text{BrNO}_6$: 514.37; Found: 513.08

2.2.3 Synthesis of fluorophore **1**



A mixture of **4** (0.2 g, 1.01 mmol), ethynylferrocene (0.28 g, 1.31 mmol), $\text{Pd}(\text{PPh}_3)_4$ (0.18 g, 0.15 mmol), PPh_3 (26.6 mg, 0.10 mmol), CuI (19.0 mg, 0.10 mmol) and triethylamine (3 mL) in toluene (3 mL) was stirred at 40°C under nitrogen atmosphere for 1.5 h. The reaction was then subjected to a typical aqueous-organic extractive work-up followed by flash chromatography using EtOAc/hexane (1:4) as the eluent to afford **1** as a dark red solid in 90% yield. Melting point $166.2 - 167.0^\circ\text{C}$ (decomposed). ^1H NMR (400 MHz, CDCl_3 , δ ppm): 8.73 (1H, d, $J = 8.9$ Hz), 8.66 (1H, d, $J = 6.8$ Hz), 8.56 (1H, d, $J = 7.2$ Hz), 7.91 (1H, d, $J = 6.6$ Hz), 7.86 (1H, s), 7.21 (2H, d, $J = 8.5$ Hz), 7.06 (2H, d, $J = 8.2$ Hz), 4.66 (2H, s), 4.38 (2H, s), 4.31 (5H, s), 4.19 (2H, s), 3.89 (2H, s), 3.75 (2H, s), 3.69 (4H, m), 3.56 (2H, s), 3.38 (3H, s). ^{13}C NMR (100 MHz, CDCl_3 , δ ppm): 164.4, 164.0, 160.9, 135.3, 134.4, 132.7, 132.5, 130.4, 129.8, 129.3, 126.5, 124.9, 124.3, 123.0, 115.7, 106.7, 89.7, 85.8, 77.8, 77.6, 77.4, 77.2, 72.4, 72.0, 71.6, 71.2, 71.1, 70.5, 69.6, 69.3, 69.1, 67.7, 59.0. MS (MALDI-TOF) Calcd for $\text{C}_{37}\text{H}_{33}\text{FeNO}_6$: 643.16 Found: 643.31

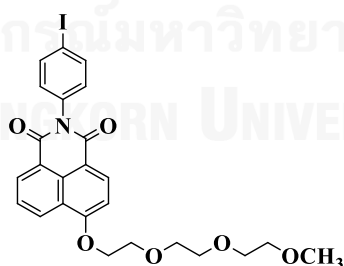
2.2.4 Synthesis of 4-bromo-*N*-(4-iodo-phenyl)-1,8-naphthalimide (5)



5

This compound was synthesized by a modified method described in the literature [60]. A mixture of commercially available 4-bromo-1,8-naphthalic anhydride (1.00 g, 3.61 mmol), 4-iodoaniline (1.58 g, 7.22 mmol), and imidazole (5.16 g, 75.8 mmol) was refluxed in CHCl_3 (30 mL). After 1.5 h, the reaction was cooled to room temperature and the solvent was removed under reduced pressure. The residue was taken up in absolute ethanol and the resulting suspension was sonicated for 15 min. A light yellow solid was filtered and dried under vacuum to afford the product (5) in 80% yield. ^1H NMR (400 MHz, CDCl_3 , δ ppm): 8.67 (1H, d, $J = 7.3$ Hz), 8.62 (1H, d, $J = 8.5$ Hz), 8.42 (1H, d, $J = 7.8$ Hz), 8.06 (1H, d, $J = 7.9$ Hz), 7.86 (1H, m), 7.04 (2H, d, $J = 8.6$ Hz). ^{13}C NMR (100 MHz, CDCl_3 , δ ppm): 163.5, 163.5, 138.6, 134.8, 133.8, 132.6, 131.7, 131.2, 130.9, 130.8, 130.6, 129.3, 128.2, 123.0, 122.1, 94.6.

2.2.5 Synthesis of 4-(2-(2-(2-methoxyethoxy)ethoxy)ethoxy)-*N*-(4'-iodophenyl)-1,8-naphthalimide (6)

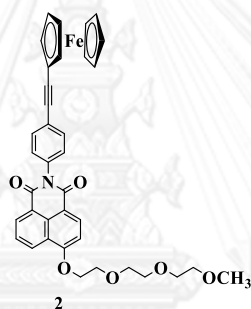


6

To a slurry mixture of NaH (60%, 0.16 g, 3.95 mmol) and anhydrous DMF (3 mL) under nitrogen atmosphere chilled in an ice bath, triethylene glycol monomethyl ether (2.84 g, 2.37 mmol) was slowly added. After the mixture was stirred for 1 h, a solution of 5 (0.38 g, 0.79 mmol) in 1 mL of anhydrous DMF was added, and the mixture was stirred while the temperature was gradually returned to room temperature for 24 h. The reaction was quenched by addition of water and the resulting solution was

extracted three times with EtOAc. The combined organic layers were sequentially washed with 5% HCl, 10% Na₂CO₃, and water. The crude product after evaporation of solvent was purified by silica gel chromatography using gradient eluents from EtOAc/hexane (1:1) to pure EtOAc to afford **6** as a yellow solid in 42% yield. ¹H NMR (400 MHz, CDCl₃, δ ppm): 8.67 (1H, d, *J* = 7.3 Hz), 8.62 (1H, d, *J* = 8.5 Hz), 8.42 (1H, d, *J* = 7.8 Hz), 8.14 (1H, d, *J* = 7.9 Hz), 7.86 (1H, m), 7.04 (2H, d, *J* = 8.6 Hz). 4.20 (2H, s), 3.90 (2H, s), 3.76 (2H, s), 3.71 (4H, s), 3.57 (2H, s), 3.40 (3H, s). ¹³C NMR (100 MHz, CDCl₃, δ ppm): 164.1, 164.0, 159.0, 133.6, 132.5, 131.7, 131.3, 130.9, 130.7, 129.5, 129.4, 128.3, 127.8, 123.4, 122.6, 115.5, 72.1, 71.0, 70.8, 70.7, 69.8, 67.8, 59.1. MS (MALDI-TOF) Calcd for C₂₅H₂₄NiO₆: 561.15 Found: 561.67

2.2.6 Synthesis of fluorophore **2**



The mixture of **6** (0.57 g, 1.11 mmol), ethynylferrocene (0.30 g, 1.44 mmol), Pd₂(dba)₃ (0.15 g, 0.17 mmol), PPh₃ (29.26 mg, 0.11 mmol), CuI (20.95 mg, 0.11 mmol) and triethylamine (3 mL) in toluene (3 mL) was stirred at 40 °C under nitrogen atmosphere for 1.5 h. After the reaction mixture was subjected to a typical aqueous-organic extractive work-up followed by flash chromatography using EtOAc/hexane (1:4) as the eluent, fluorophore **2** was obtained as a yellow solid in 96% yield. Melting point 155.4 – 155.8 °C (decomposed). ¹H NMR (400 MHz, CDCl₃, δ ppm): 8.67 (1H, d, *J* = 7.3 Hz), 8.62 (1H, d, *J* = 8.5 Hz), 8.42 (1H, d, *J* = 7.8 Hz), 8.06 (1H, d, *J* = 7.9 Hz), 7.86 (1H, m), 7.23 (2H, d, *J* = 8.5 Hz), 7.08 (2H, d, *J* = 8.2 Hz), 4.67 (2H, s), 4.40 (2H, s), 4.32 (5H, s), 4.20 (2H, s), 3.90 (2H, s), 3.76 (2H, m), 3.71 (4H, m), 3.57 (2H, m), 3.38 (3H, s). ¹³C NMR (100 MHz, CDCl₃, δ ppm): 164.4, 164.0, 160.9, 135.3, 134.4, 132.7, 132.5, 130.4, 129.8, 129.3, 126.5, 124.9, 124.3, 123.0, 115.7, 106.7, 89.7, 85.8, 77.8, 77.6, 77.4, 77.2, 72.4, 72.0, 71.6, 71.2, 71.1, 70.5, 69.9, 69.3, 69.1, 59.5. MS (MALDI-TOF) Calcd for C₃₇H₃₃FeNO₆: 643.16 Found: 642.99

2.3 Measurement of UV-Vis and fluorescence spectra

Stock solution of compound **1** and **2** (100 μM) were prepared in acetonitrile. Stock solutions (10mM) were prepared in deionized water by dissolving of perchlorate, acetate, chloride or nitrate form of Ag (I), Au (I), Au (III), Bi (III), Ca (II), Cd (II), Co (II), Cr (II), Cu (II), Fe (III), Ga (III), Hg (II), Mn (II), Ni (II), Pb (II), Sr (II) and Zn (II) ions except for HAuCl_4 for Au (III) ions.

In typical experiment, test solutions were prepared by placing 50 μL of the probe stock solution into 2.0 mL Eppendorf[®] tube, adding an aliquot of each metal stock, then dilute the solution to 1.0 mL with 10 mM PBS (pH 8.0) and acetonitrile. Normally, excitation was at 369 nm. Both excitation and emission slit widths were 5 nm. Fluorescence spectra were measured after addition of Au (III) 15 min. For low concentration of Au (III), fluorescence spectra were measured after addition of Au (III) for 30 min.

2.4 Interference behaviors from other metal species on Au (III) signaling

Under the same measurement conditions, competitive signaling behavior of probe **2** toward Au (III) ions in the presence of coexistence metal ions as background were studied. Final concentration of **2**, Au (III), and the other various competing metal ions were 5 μM , 20 μM and 0.2 mM, respectively, in CH_3CN -PBS buffer (pH 8.0, 10 mmolL^{-1} , 4/6, v/v).

2.5 Water content effect on reaction time and Au (III) signaling

The water effect of probe **2** on Au (III) signaling investigated by measuring of fluorescence emission spectra at 467 nm and reaction time at highest fluorescence intensity in series of water/acetonitrile was 4/6 to 8/2 (v/v). The sample solution with different water content in acetonitrile were freshly prepared prior each measurement. Final concentrations of probe and Au (III) and each buffer solution were 5 μM and 0.5 mM, respectively.

2.6 pH effect on Au (III) signaling

The pH effect on Au (III) signaling of probe **2** was investigated by measuring of fluorescence emission spectra in the series of buffer between pH 4.0-9.0. The pH of the solution was fixed by using acetate buffer (pH 4.0-6.0), phosphate (7.0-8.0) and tris-HCl (9.0). Final concentrations of probe, Au (III) and each buffer solution were 5 μM , 0.5 mM and 10 mM, respectively, in CH_3CN -PBS buffer (pH 8.0, 10 mmol^{-1} , 4/6, v/v).

2.7 Surfactant effect on Au (III) signaling

The surfactant effect on Au (III) signaling of probe **2** was investigated by measuring of fluorescence emission spectra with three types of surfactant; cationic (TTAB and CTAB), anionic (Tween-20, Brij and Triton X-100) and non-ionic (SDBS) surfactant. Final concentrations of probe and Au (III) were 5 μM and 0.5 mM, respectively. Concentration each surfactant solution was used at its CMC point. All experiments were carried in CH_3CN -PBS buffer (pH 8.0, 10 mmol^{-1} , 4/6, v/v). Under same measurement conditions.

2.8 Limit of detection

The limit of detection of fluorophore was estimate by plotting of fluorescence change of probe **2** in the presence of Au (III) (0.0-3.0 μM , HAuCl_4 as Au (III) source) as a function of fluorescence intensity (taken as peak height at 467 nm) following the reported procedure [61]. Also, the minimum concentration of Au (III) that gives the fluorescence intensity was determined with a signal-to-background ratio of three.

2.9 Elucidation of sensing mechanism by ^{13}C -NMR spectroscopy

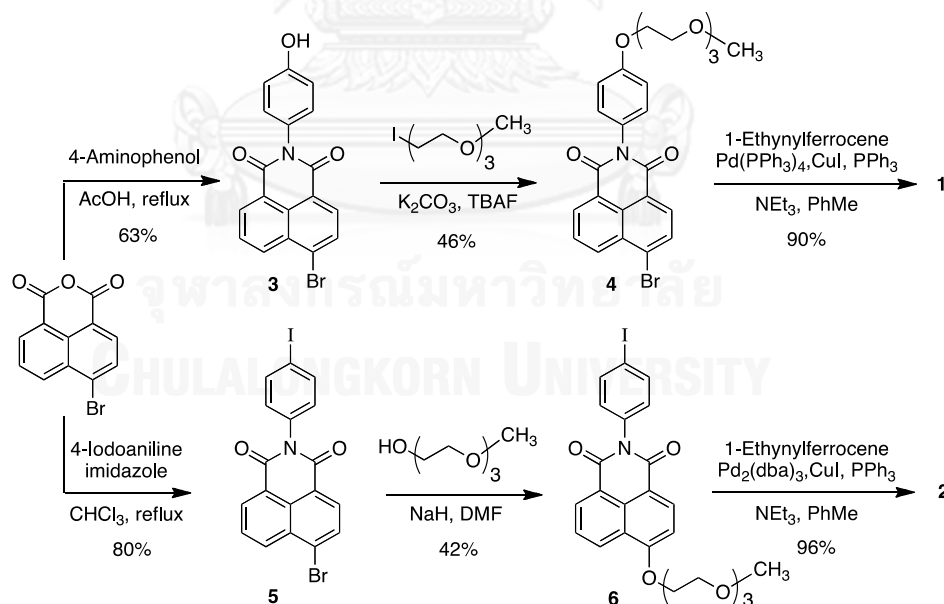
To have evidence for the complexation between Au (III) and **2**, the ^{13}C -NMR spectra **2** and the reaction product of **2** with HAuCl_4 were obtained. To a solution of **2** (70 mM, in CD_3CN) was added HAuCl_4 solution, and the mixture was mixed properly at room temperature. The final concentration of **2** and HAuCl_4 is 60 mM and 0.15 mM, respectively. The ^{13}C -NMR spectra of compound **2** and the reaction product of **2**-Au (III) were measured in CD_3CN .

CHAPTER III

RESULTS AND DISCUSSION

3.1. Synthesis and characterization of fluorophores

The synthesis of our fluorophores began with an imidation of commercially available 4-bromo-1,8-naphthalic anhydride (**Scheme 3.1**). Refluxing of such compound with *p*-aminophenol in glacial acetic acid provided naphthalimide **3** in 63% yield, whereas the reaction with *p*-iodoaniline and imidazole in CHCl₃ yielded naphthalimide **5** in 80% yield. The installation of a hydrophilic triethylene glycol group into **3** was carried out by *O*-alkylation of the phenolic –OH group using 1-iodo-2-(2-(2-methoxyethoxy)ethoxy)ethane under basic condition. Meanwhile, a nucleophilic aromatic substitution of the bromine in **5** by triethylene glycol monomethyl ether in the presence of NaH afforded **6** in 42% yield. Finally, the Sonogashira coupling with ethynyl ferrocene transformed **4** and **6** into target compound **1** as reddish solid in 26% total yield (3 steps) and **2** as yellowish solid in 32% total yield (3 steps). All of the compounds were then fully characterized by ¹H-NMR spectroscopy (**Figure 3.1** and **3.2**). The physical appearance, ¹H-NMR (**Figure 3.3** and **3.4**) and its ¹³C-NMR, IR and mass spectrometry of target compound **1** and **2** are shown in appendix.



Scheme 3.1 Synthesis of **1** and **2**.

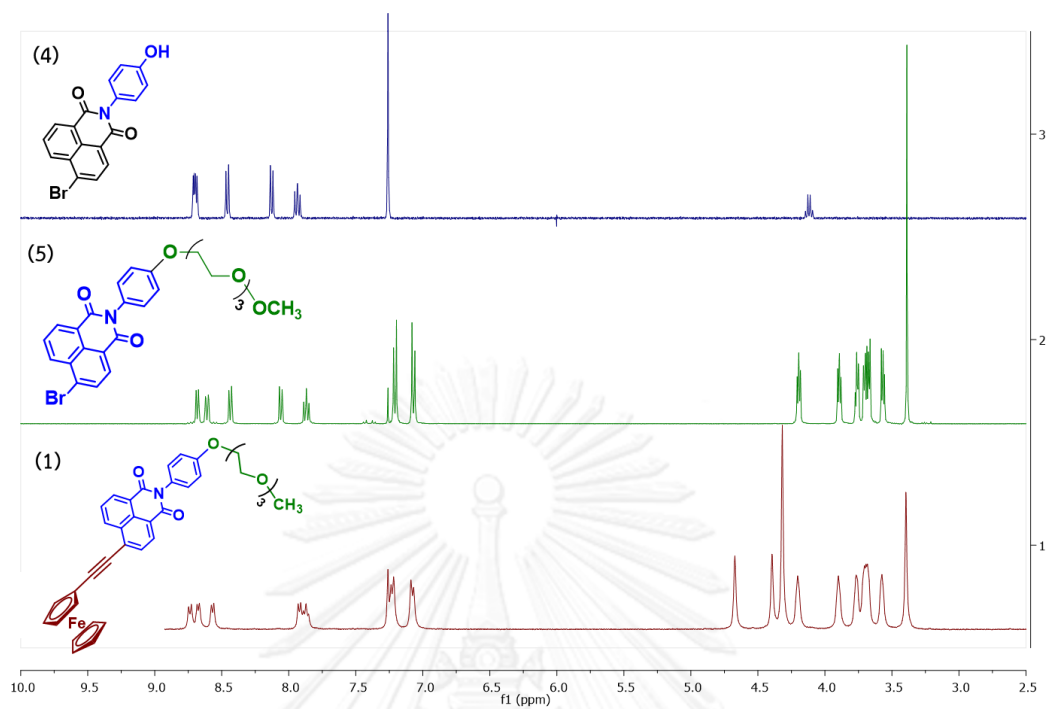


Figure 3.1 The comparison of $^1\text{H-NMR}$ of compound 3, 4 and 1.

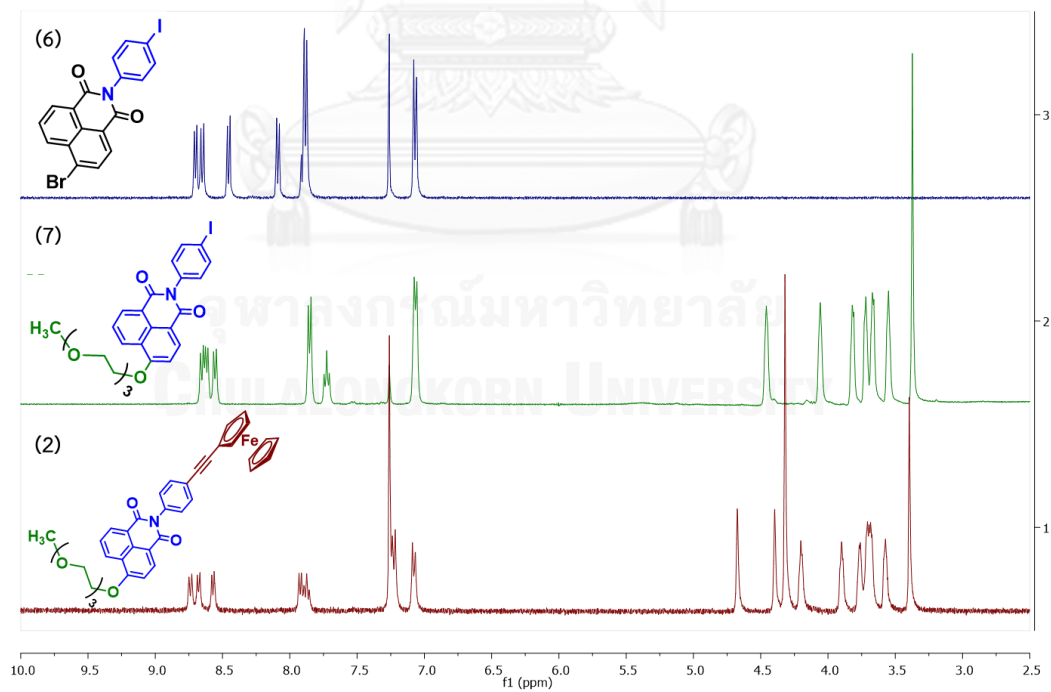


Figure 3.2 The comparison of $^1\text{H-NMR}$ of compound 5, 6 and 2.

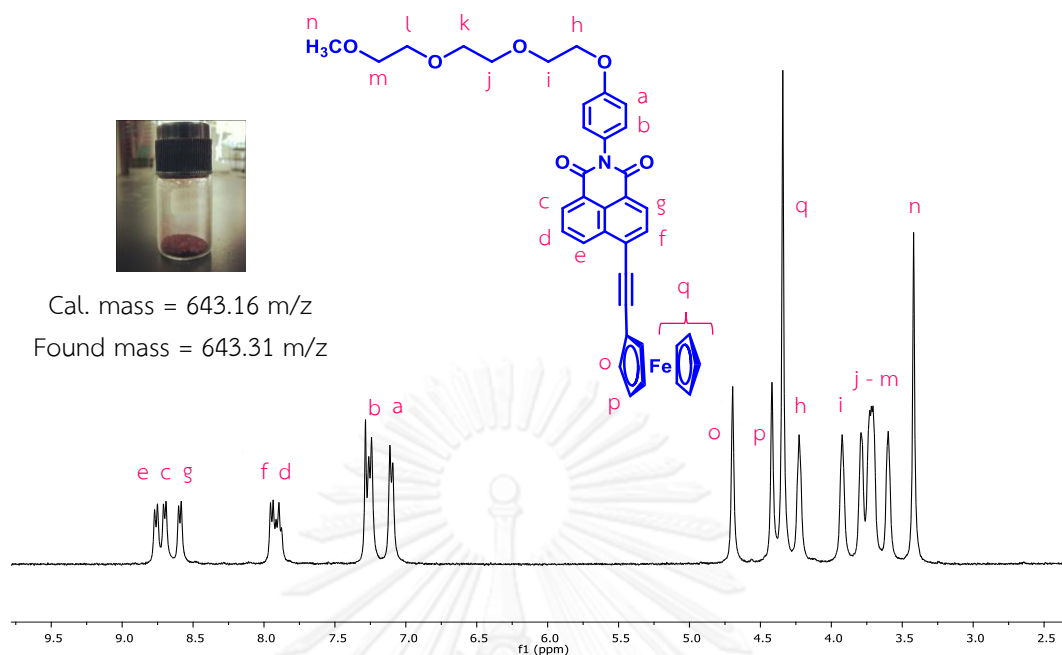


Figure 3.3 The physical appearance, mass spectroscopic analysis and $^1\text{H-NMR}$ of compound 1.

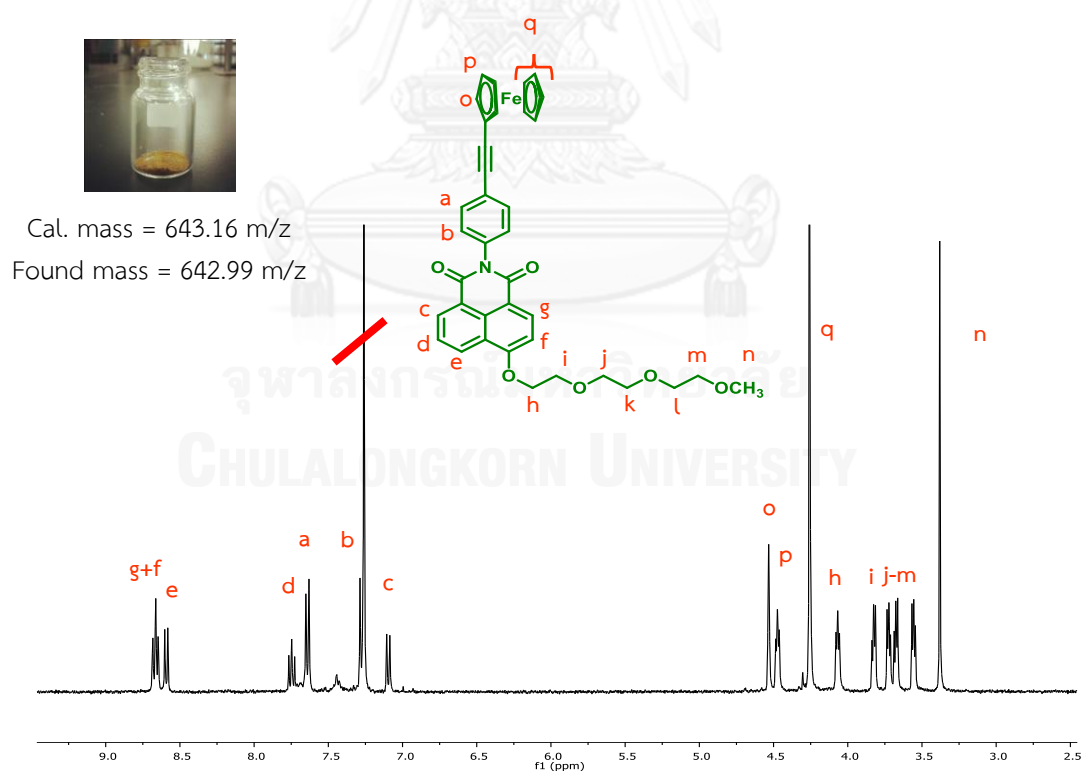


Figure 3.4 The physical appearance, mass spectroscopic analysis and $^1\text{H-NMR}$ of compound 2.

3.2. Photophysical properties of fluorophores

The photophysical properties of **1** and **2** were investigated using their solutions in 1:1 mixture between CH₃CN and H₂O. The results are tabulated in **Table 3.1** and the normalized absorption and emission spectra are shown in **Figure 3.3**.

Table 3.1 Photophysical properties of **1** and **2** in CH₃CN–H₂O (v:v = 1:1).

Compound	Absorption		Emission		Stokes shift (cm ⁻¹)
	λ_{\max} (nm)	ϵ (M ⁻¹ cm ⁻¹)	λ_{\max} (nm)	Φ^a_{F}	
1	380	9000	405	<0.01	1624
2	369	17,000	453	0.01	5025

^aquinine sulfate in 0.1 M H₂SO₄ ($\Phi = 0.54$) was the reference.

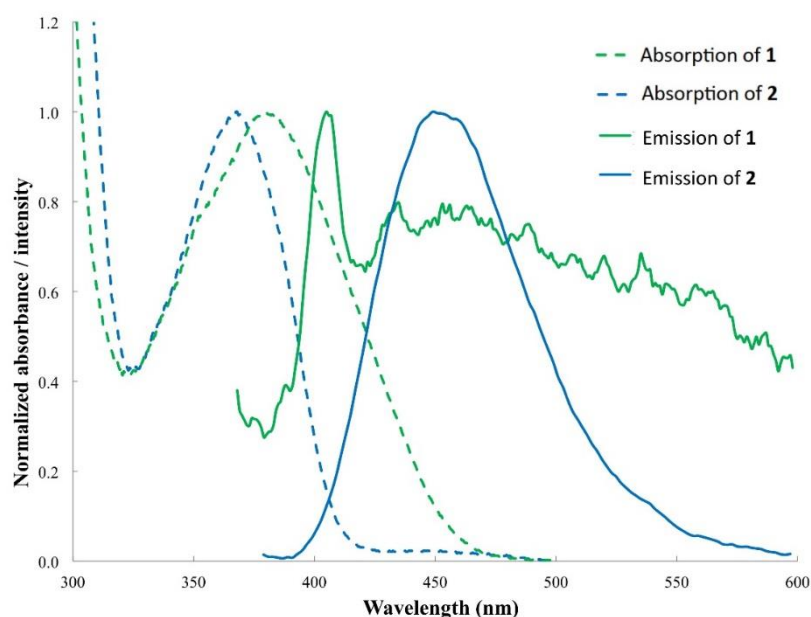


Figure 3.5 Normalized absorption (solid line) and emission spectra (dashed line) of 1,8-naphthalimide **1** and **2** in CH₃CN–H₂O (1/1; v/v).

For the absorption, **1** and **2** showed a maximum absorption wavelength at 380 nm and 369 nm, respectively. The longer maximum absorption wavelength of **1** corresponds to a longer conjugated system caused by the extension of pi-system of the 1,8-naphthalimide fluorophore by the ethynylferrocene appended at the

4-position. The substitution at this position by a heteroatom such as O in **2** leads to the compounds with absorption around 360-370 nm [62].

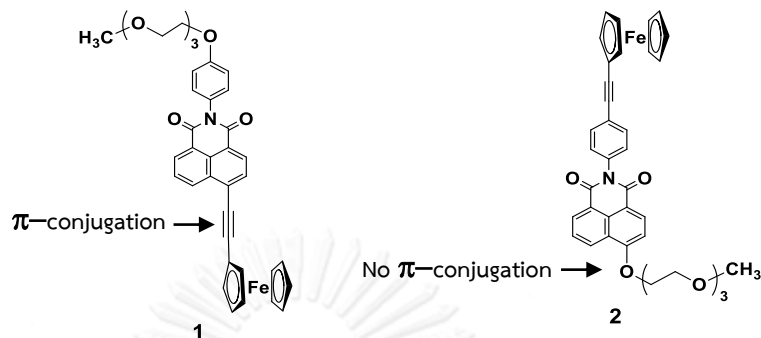


Figure 3.6 Representative of π -conjugation at 4-position of **1** and **2**.

From the molar extinction coefficient data, **2** appears to be a more absorptive compound than **1**. This might correspond to the absorption of light in **2** that generates a charge transfer interaction between the substituent at 4-position and the imide carbonyl group as depicted in Figure 3.5 [63].

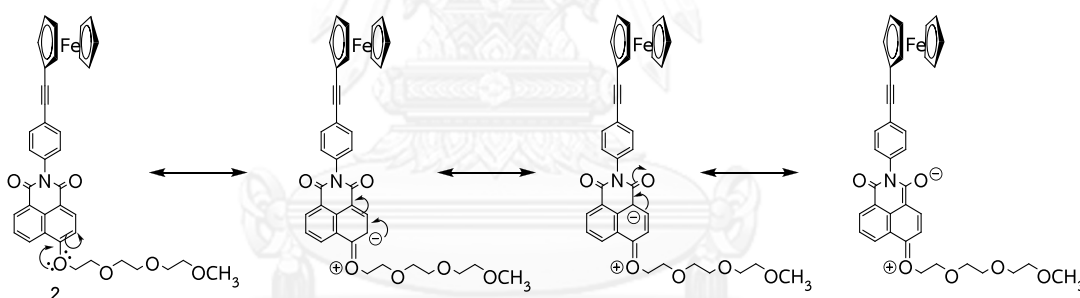


Figure 3.7 Proposed charge separation in **2**.

For the fluorescence data, **1** shows maximum emission wavelength at 405 nm. Compound **2**, on the other hand, exhibits maximum emission wavelength at 453 nm in the blue region which is generally characteristic electron transition in the naphthalimide derivatives with halogen or good electron-donating alkoxy group at C-4 position (Figure 3.6) [38].

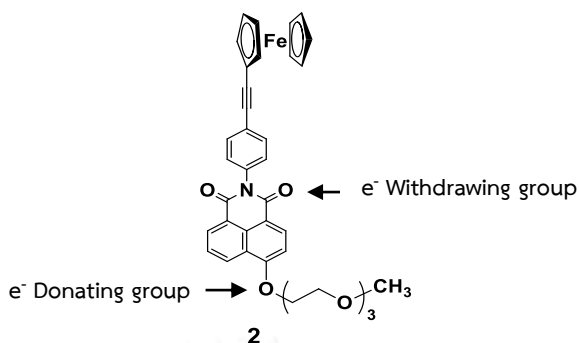


Figure 3.8 Electron donating and withdrawing in 2.

The Stokes shift values of **1** and **2** were calculated to 1624 and 5025 cm^{-1} , respectively. The larger Stokes shift in **2** corresponds to the presence of an electron-donating (alkoxy group) and withdrawing groups (carbonyl group) in the structure causing an ICT process (Figure 3.7). Polar solvents such as a mixture of CH_3CN and H_2O can stabilize the excited molecule with a charge separation and also lower the energy of the lone pair electrons by a strong H-bond formation. In addition, a larger geometry difference between its excited state and ground state may result from various modes of vibration and rotation of the triethylene glycol unit attached to the fluorophore pendant. This large Stokes shift is a prominent point for fluorescent sensor applications since it could prevent self-absorption between the emission and the excitation.

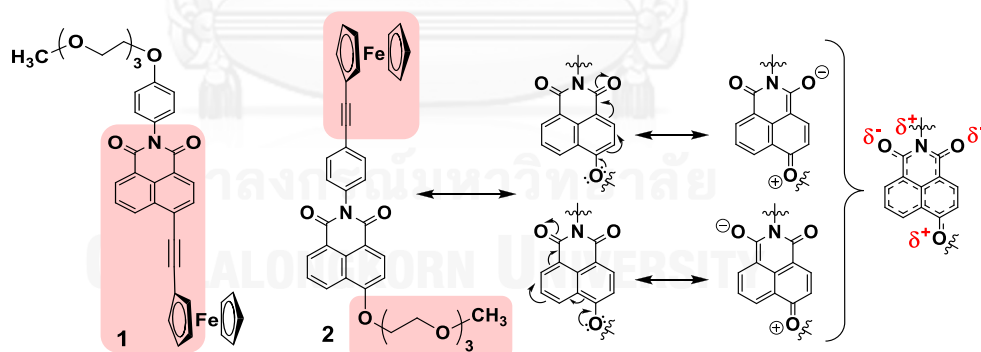


Figure 3.9 Rational description of low fluorescence emission of **1** and **2**.

The efficiency of molecule to emit of the absorbed light energy is characterized by the fluorescence quantum yield. As expected, both 1,8-naphthalimide derivatives exhibit unusually low quantum efficiency, in the comparison with the parent 1,8-naphthalimide, due to the effect of the fluorescence quenching process (PET) from

ethynyl ferrocene to the excited state of naphthalimide part. However, the fluorescence quantum yield of **1** cannot be determined since its signal is extremely low. For compound **1**, there is a direct conjugation between naphthalimide and one of the cyclopentadienyl ligands (**Figure 3.7, left**). Thus, there might be a possibility for metal to ligand charge transfer (MLCT) or ligand to metal charge transfer (LMCT) that leads to a non-emissive behavior.

For compound **2**, the fluorescence emission can be observed under the same conditions with a low quantum efficiency of around 1%. This weakly fluorescent property may cause by the combination of ICT effect between the electron donor at the 4-position to naphthalimide and the carbonyl group, as well as the through-space PET effect by the ferrocenyl group (**Figure 3.7, right**).

3.3. Selectivity screening of compound **1** and **2** toward various metal cations in aqueous media.

With both **1** and **2** in our hands, the selectivity of these compounds toward various metal ions were investigated by monitoring their fluorescent signal changes in the presence of Ag (I), Al (III), Au (I), Au (III), Bi (III), Ca (II), Cd (II), Co (II), Cr (II), Cu (II), Fe (III), Ga (III), Hg (II), Mn (II), Ni (II), Pd (II), Pb (II), Sr (II) and Zn (II) in aqueous media.

In the case of **1**, no significant change in fluorescent signal was found in the presence of metal ions examined (Figure 3.8). However, the signal of **2** was enhanced to approximately 8 and 2 folds of its original intensity in the presence of Au (III) and Au (I), respectively (Figure 3.9 and 3.10).

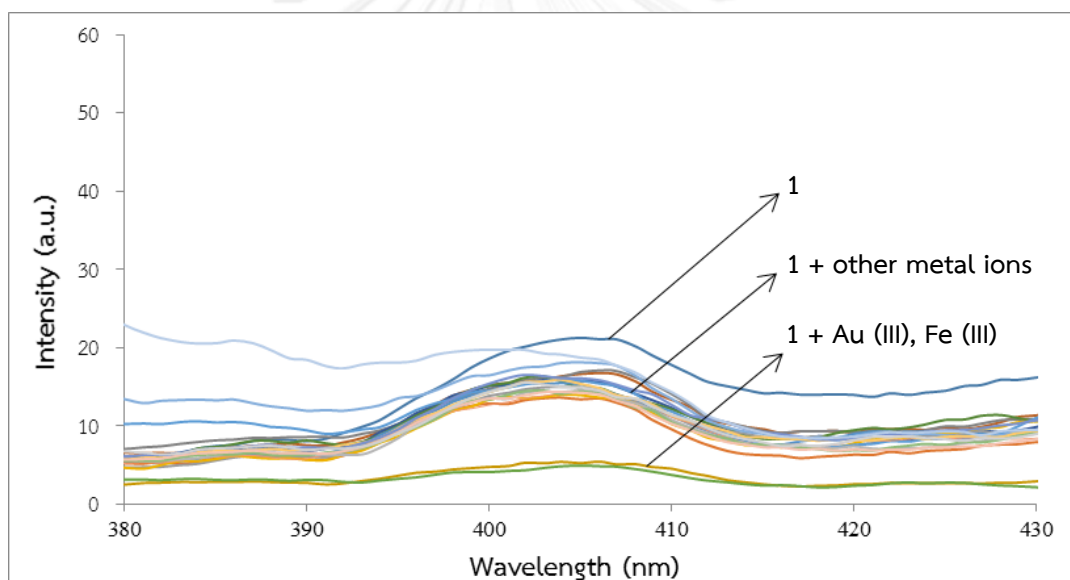


Figure 3.10 Fluorescence spectra of compound **1** (5 μM , λ_{ex} 369 nm) in a mixture of CH_3CN -PBS buffer solution (pH 8.0, 10 mM, 1/1, v/v) upon addition of various metal ions (0.5 mM).

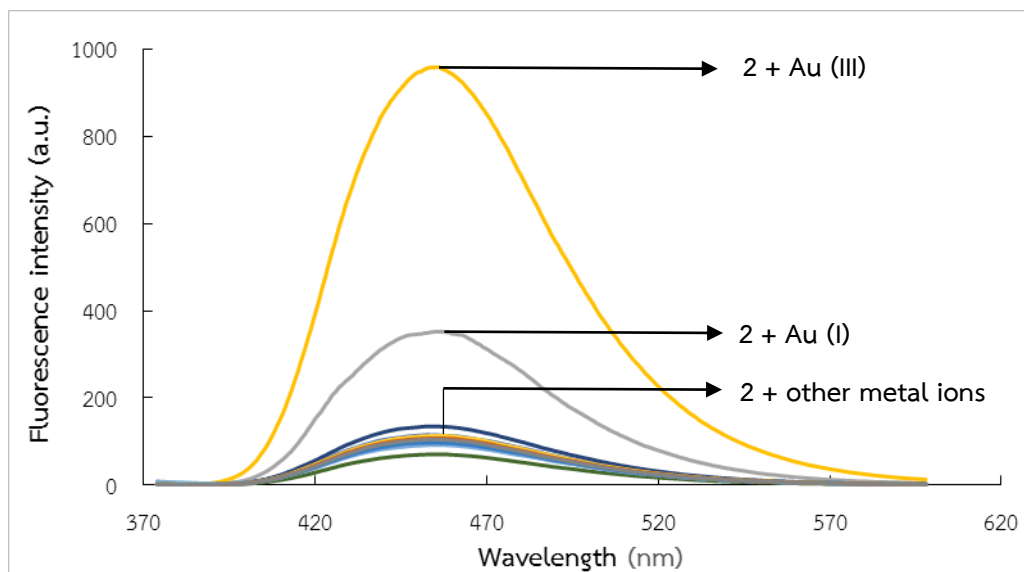


Figure 3.9 Fluorescence spectra of compound **2** ($5 \mu\text{M}$, λ_{ex} 369 nm) in a mixture of CH_3CN -PBS buffer solution (pH 8.0, 10 mM, 1/1, v/v) upon addition of various metal ions (0.5 mM).

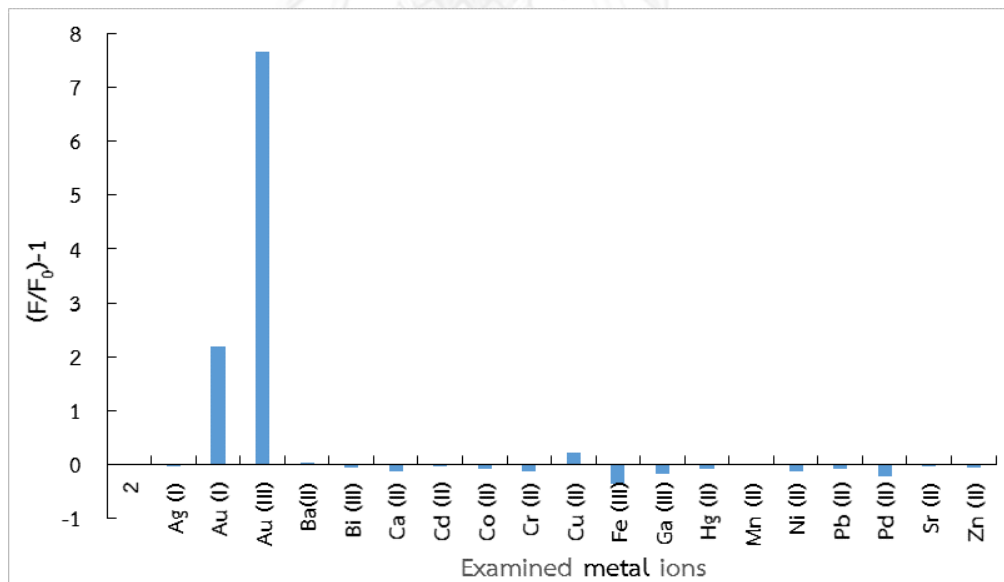
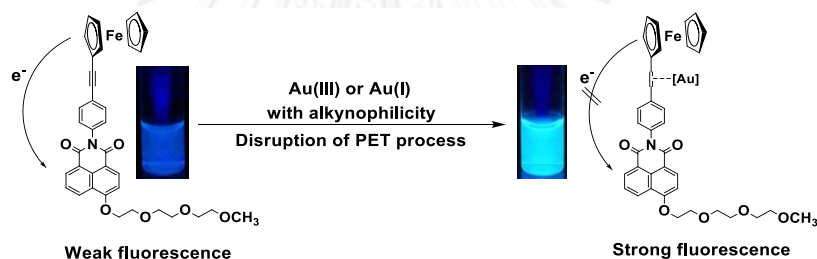


Figure 3.10 Relative fluorescence responses at λ_{em} 456 nm, where F is the fluorescence intensity in the presence of metal ion analyte and F_0 is the original fluorescent intensity of **2**. [Inset: fluorescence spectra of **2** ($5 \mu\text{M}$, λ_{ex} 369 nm) in a mixture of CH_3CN -PBS buffer solution (pH 8.0, 10 mM, 1/1, v/v) upon addition of various metal ions (0.5 mM)].

3.4. Elucidation of the proposed sensing mechanism of compound **2** toward gold ions.

This selectivity towards gold ions is attributed to the special alkynophilicity of the gold ions toward the triple bond. For compound **1**, the complexation of Au species to the triple bond may not completely disturb the conjugation between fluorophore and ferrocene group because the complexation usually exploits one of the two pi-bonds, leaving another bond to maintain the conjugation. Therefore, the PET process could still take place after the complexation.

For compound **2** which does not possess a direct conjugation between naphthalimide and ferrocene groups, the through-space PET process could be somewhat disturbed after alkyne-Au complexation. On the basis of these fluorescence quenching process, the fluorescence signal can be enhanced when the coordination of the gold ion at the triple bond occurs. The proposed sensing mechanism is shown in Scheme 3.2.



Scheme 3.2 Proposed sensing mechanism of **2** towards Au (III) or Au (I) ion.

To elucidate these proposed sensing mechanism, we decided to use ^{13}C -NMR spectroscopy technique for monitoring the change of alkynyl-carbon of compound **2** in the absence and the presence of Au (III). The results were shown in Figure 3.11 and 3.12. It is clear that the addition of Au (III) caused the disappearance of alkynyl-carbon signals at 90 and 85 ppm, even after 10,000 scans. This data supports our proposed sensing mechanism to some extents.

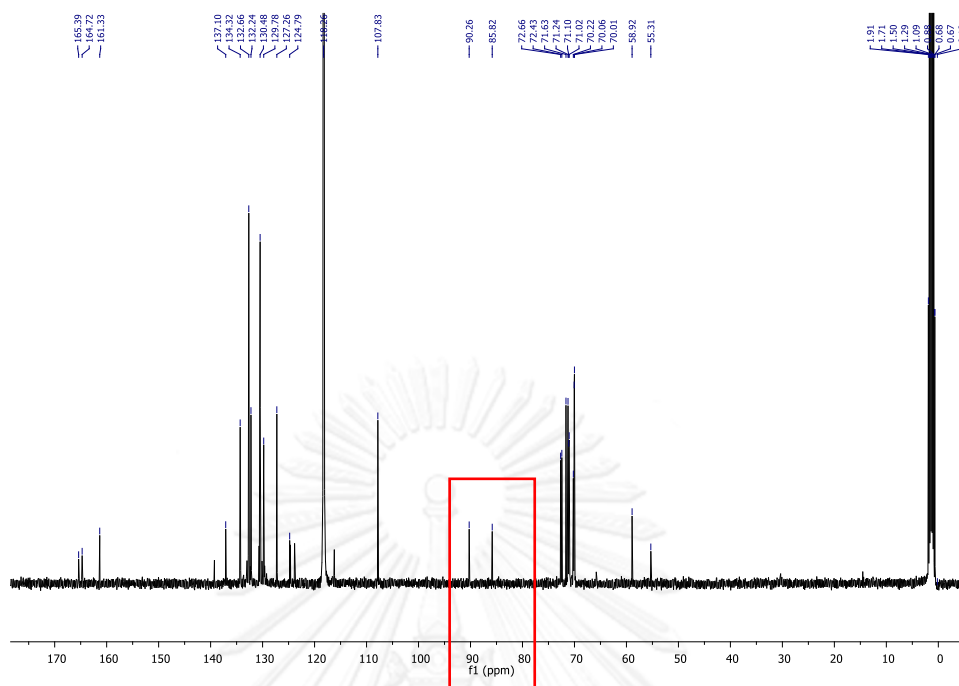


Figure 3.11. ^{13}C -NMR (400 MHz) of compound 2 (70 mM) in CD_3CN (3,000 scans).

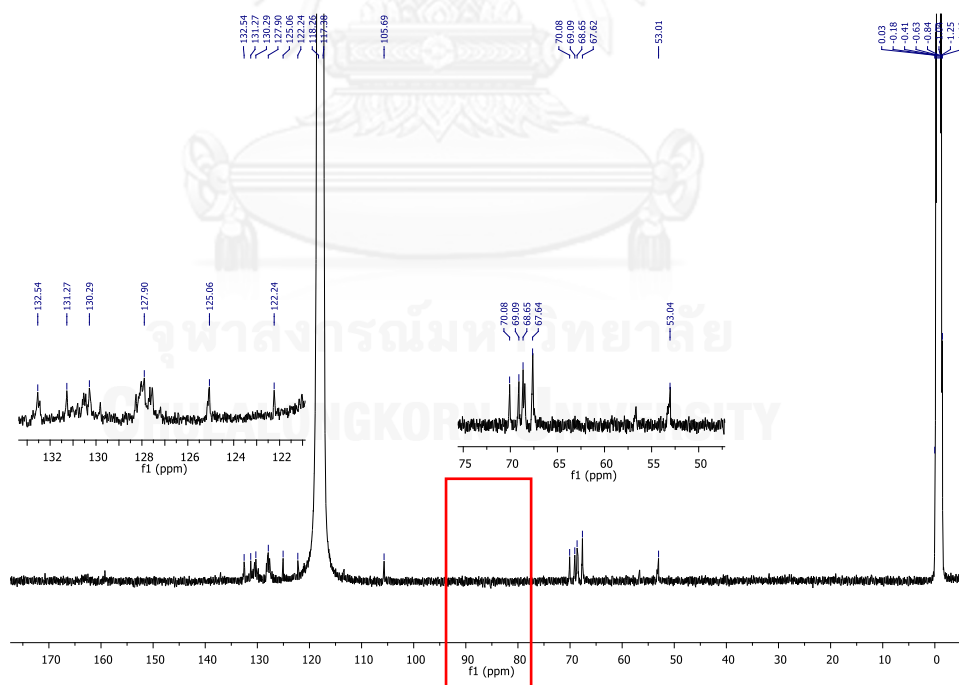


Figure 3.12. ^{13}C -NMR (400 MHz) of compound 2 (60 mM) with Au (III) 0.15 mM in CD_3CN (10,000 scans).

3.5. Optimization of sensing conditions of compound **2** towards Au (III)

The conditions in which fluorescent sensors operate usually affect their performance. Besides high selectivity, a short response time is strongly considered for a fluorescent sensor to monitor target metal in environmental samples in real time. In our study, the effect of water content in acetonitrile on selectivity and response time was first investigated.

It should be noted that, the fluorescence enhancement of **2** in a mixture of CH₃CN-H₂O (1/1, v/v) depends on the amount of the gold ion. Typically, when 10 eq. of Au (III) was used, the fluorescence intensity gradually increased and saturated within 2 h. For a faster measurement, higher concentration of Au (III) must be used. For example, the fluorescence intensity was enhanced within 15 min when 100 eq. of Au (III) was used. **Table 3.2** summarizes the data on the enhanced fluorescent intensity and the time required to reach a constant intensity (response time) under the various ratios of water and CH₃CN.

Table 3.2. Effect of water content on fluorescence intensity of compound **2** towards Au (III) ion

Entry	Volume ratio of water in CH ₃ CN	Without Au(III)	With Au(III)		F/F ₀
		F ₀ (a.u.)	F (a.u.)	T _F (min)	
1	0.1 : 0.9	86.2	417.9	>60	4.8
2	0.2 : 0.8	85.1	600.7	50	7.1
3	0.3 : 0.7	84.2	671.3	40	8.0
4	0.4 : 0.6	85.7	715.6	40	8.4
5	0.5 : 0.5	85.5	734.6	30	8.6
6	0.6 : 0.4	82.2	751.0	15	9.1
7	0.7 : 0.3	124.5	696.4	10	5.6
8	0.8 : 0.2	111.3	621.0	10	5.6

Measurement conditions: [**2**] = 5 μM and [Au(III)] = 0.5 mM in CH₃CN-PBS (pH 8.0, 10 mM) (λ_{ex} 369 nm, λ_{em} 456 nm)

When the data from **Table 3.2** was transformed into **Figure 3.13**, it is obvious that the fluorescence intensity of **2** in the presence of Au (III) were gradually increased when the fraction of aqueous in CH₃CN increase from 0.1 to 0.5, and reached a maximum point when the aqueous fraction was 0.6. In addition, the aqueous fraction of 0.6 could also offer the highest fluorescence enhancement (9.1 fold, blue triangle) in a practicable experimental time of 15 min (orange circle). When this aqueous fraction is raised to 0.7 and 0.8, the enhanced fluorescence intensities were obviously lower. The increase in water content was not only increase the polarity of solutions, it also promotes the hydrogen bonding between solvents and carbonyl groups of naphthalimide (which acts as H-bonding acceptor), which in turn stabilizes the geometry of the excited state and yields a weaker fluorescence signal. Therefore, this mixture of solvents at 0.6 aqueous fraction was selected for further optimization study.

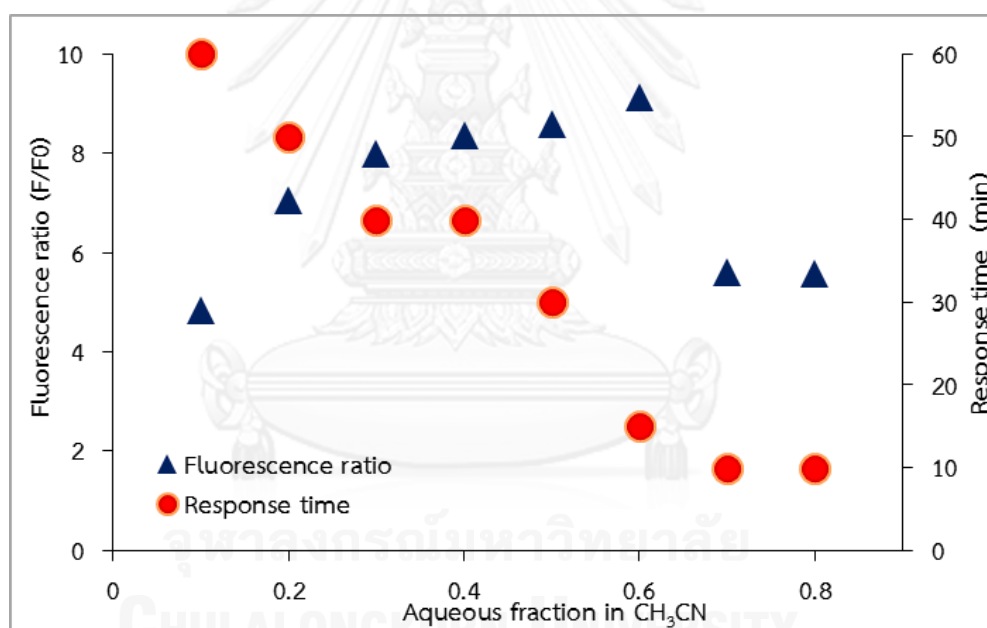


Figure 3.13. Fluorescence intensity change and saturate time of compound **2** (5 μM) with Au (III) (500 μM) in the mixture of PBS buffer—CH₃CN in various fraction ($\lambda_{\text{ex}} = 367$ nm).

Next, the effect of pH of the media on the enhanced fluorescent signal was examined (**Figure 3.14**). We carried out a series of experiments using solutions of **2** in 6/4 (v/v) mixture of aqueous buffer solution at various pH and CH₃CN (acetate buffer for pH 4 to 5, phosphate buffer for pH 6.0 to 8.0, and tris-HCl buffer for pH 9.0). Upon addition of Au (III), the fluorescent signals were enhanced to a saturated level within 15 minutes for every conditions, but the levels of enhancement depended on the pH of the buffer. Results indicated that the best sensitivity of the Au (III) detection by **2** could be achieved at pH 7 to 8.

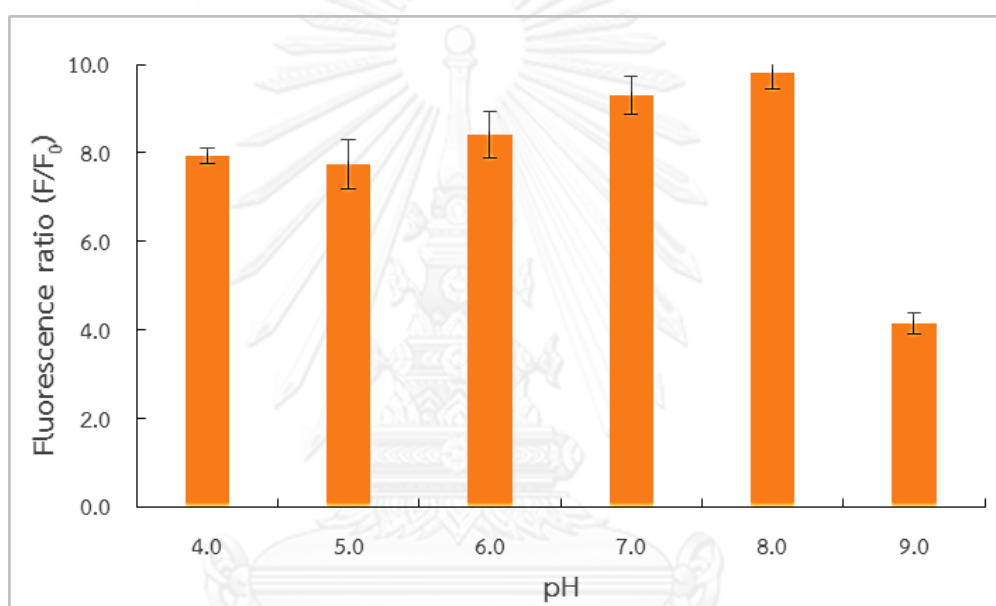


Figure 3.14. Fluorescent enhancement of **2** (5 μ M) by Au (III) (50 mM) at various point of pH.

There are several examples on the use of surfactants to improve the sensitivity of aqueous-based chemosensors [64-67]. In this study, the emission enhancement behavior of **2** by Au (III) was investigated using a variety of surfactants at the concentration above their critical micelle concentration (CMC), for example anionic (SDBS), cationic (TTAB and CTAB) and non-ionic (Brij and Triton X-100). **Figure 3.15.** showed that the enhanced signals worsen when the cationic surfactants were used. However, both non-ionic and anionic-type surfactants could not improve the sensitivity since there was no significant difference fluorescence ratio compare to sample which is without any surfactant.

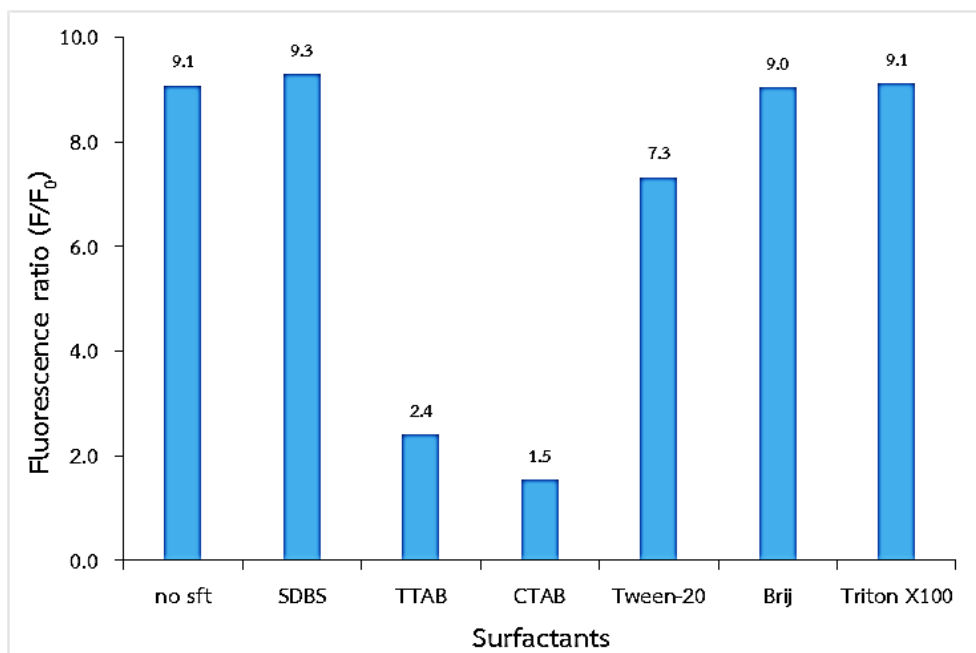


Figure 3.15 Relative fluorescence responses of **2** (5 μM) with Au (III) (0.5 mM) in the presence of various surfactants (near CMC point of each surfactant) in CH_3CN and 10 mM PBS buffer pH 8.0 (4/6, v/v). All fluorescent intensities were acquired 15 minutes after the addition of Au (III) and surfactants, respectively. ($\lambda_{\text{ex}} = 367 \text{ nm}$).

3.6 Selectivity and sensitivity determination of compound **2** towards Au (III)

The interference of other metal ions in Au (III) detection was examined using solutions of **2** (5 μM), Au (III) (20 μM), and each of the interfering ion at 10-fold concentration of Au (III) (200 μM) (**Figure 3.16**). With the exception of Fe (III), other interfering ions did not cause significant differences in fluorescent signal in the presence of Au (III). The interference by Fe (III) may result from the filtering effect as the ferric ion possesses a significant absorption in the absorption range of **2** [68]. In the case of Hg (II) ions can activate the alkynes, as well as Pd (II), especially terminal-alkynes [25, 69], so we designed the probe with non-terminal alkyne. Unfortunately, the effect from Hg (II) ion still remained.

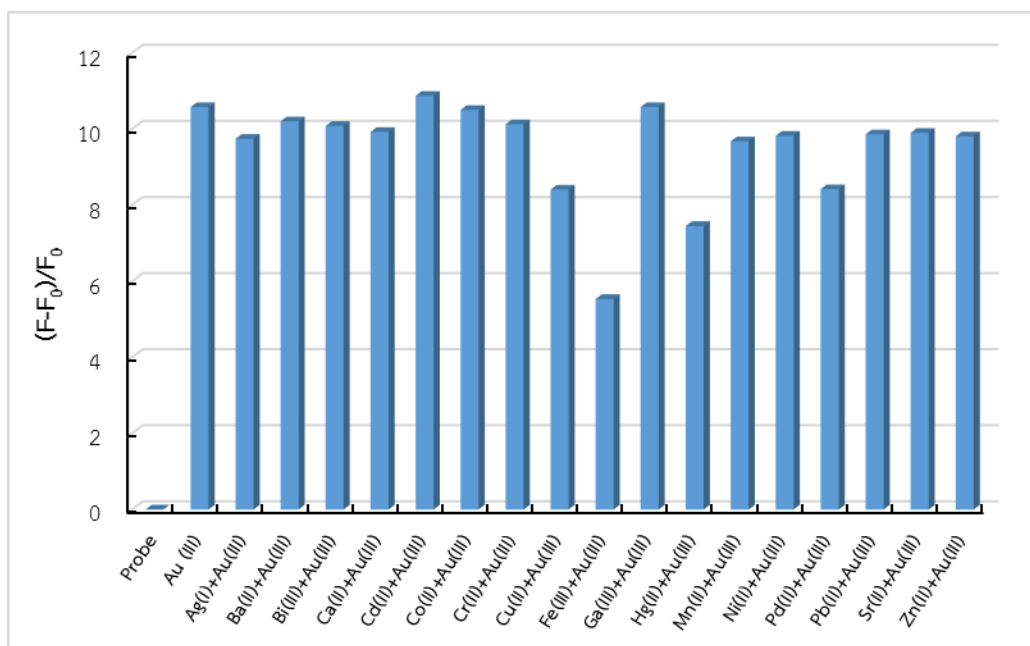


Figure 3.16. Relative fluorescence responses of **2** (5 μM) with Au (III) (20 μM) in the presence of various metal ions (200 μM) in CH_3CN and 10 mM PBS buffer pH 8.0 (4/6, v/v). All fluorescent intensities were acquired 15 minutes after the addition of Au (III) and interfering ions. ($\lambda_{\text{ex}} = 367 \text{ nm}$).

In order to determine the detection limit, we treated compound **2** (1 μM) with 0.00 to 3.00 μM of Au (III) in mixture of PBS buffer solution (10 mM, pH 8.0) in CH_3CN (6/4, %v/v) then its fluorescence spectra were taken after 1h at same measurement conditions. It should be noted that for a faster measurement, more than 1 μM can be used. For example, the fluorescence saturation was attained within 15 min when 5 μM of compound **2** were used. Results were showed in **Table 3.3**.

Then, we constructed a plot between fluorescent signal and concentration of Au (III) as shown in **Figure 3.17**. From the linearity obtained in the concentration range between 0.5 and 3.0 μM , the limit of detection of three-times-noise [61] was determined to be $4.0 \times 10^{-4} \mu\text{M}$ or 80 ppb. Then, the calculations are shown.

Table 3.3. Fluorescence intensity of **2** (1 μM) when treated with 0.00 to 3.00 μM of Au (III) in mixture of PBS buffer solution (10 mM, pH 8.0) in CH_3CN (6/4, v/v).

[Analyte] (μM)	Average fluorescence intensity (a.u.)	SD
0.00	19.72	1.24
0.50	42.76	5.45
1.00	79.73	6.53
1.50	98.65	5.41
2.00	121.08	3.22
2.50	142.11	6.65
3.00	159.34	4.32

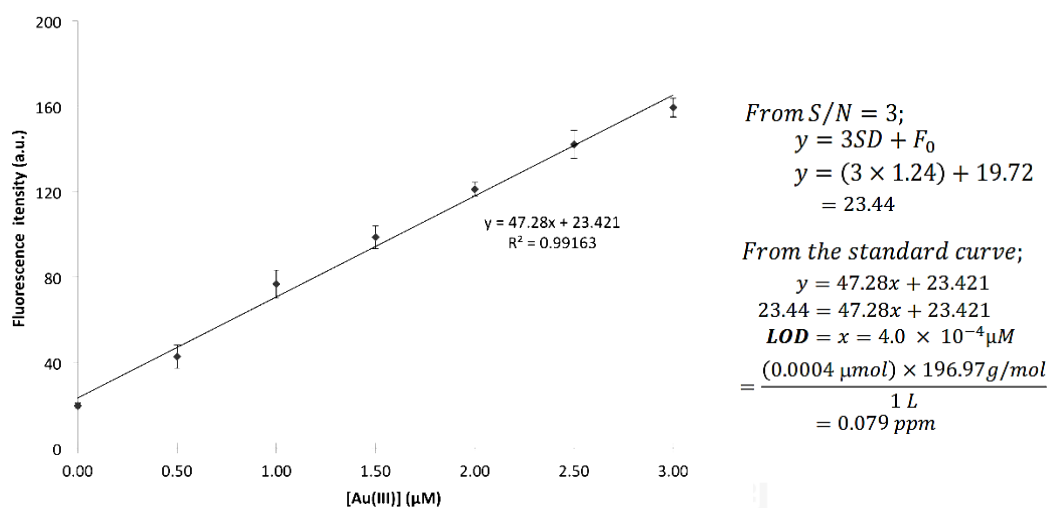


Figure 3.17. Fluorescence response of **2** (1 μM) in CH_3CN -PBS buffer pH 8.0, 10 mM, (4/6, v/v) when treated with 0 – 3 μM of Au (III) ($\lambda_{\text{ex}} = 367 \text{ nm}$; $\lambda_{\text{em}} = 467 \text{ nm}$, measured after 15 minutes) and calculation of the limit of detection (LOD).

CHAPTER IV

CONCLUSIONS

In conclusions, two new *N*-aryl-1,8-naphthalimides containing an ethynylferrocene and triethylene glycol monomethyl ether chain were successfully synthesized from the commercially available 4-bromo-1,8-naphthalic anhydride with appropriated aniline derivatives. The installation of triethylene glycol chain was for improving their solubilities in aqueous solution. The incorporation of an ethynylferrocene relied on the Sonogashira coupling reaction. Both of these compounds were fully characterized by various spectroscopic techniques.

The investigation of their photophysical properties show the maximum absorption wavelengths around 360-370 nm. The larger stoke shift in **2** corresponds to the presence of an electron-donating and withdrawing groups in the structure causing an ICT process. While compound **1** is virtually non-emissive due to the MLCT or LMCT, compound **2** exhibits the maximum emission wavelength in the blue region which is generally characteristic electron transition in the naphthalimide derivatives with halogen or good electron-donating alkoxy group at C-4 position. However, as expected, its quantum efficiency is relatively low due to the PET effect from ethynyl ferrocene to naphthalimide part.

The selectivity investigation of these fluorophores indicated that compound **2** shows a selective fluorescent enhancement by Au (III) or Au (I) ions. This selectivity towards gold ions is attributed to the special alkynophilicity of the gold ions toward the triple bond as proven by ¹³C-NMR experiments. The conditions in which fluorescent sensors operate were optimized. In this study, the aqueous fraction of 0.6 in acetonitrile with pH 7-8 could also offer the highest fluorescence enhancement (9.1 fold) in a practicable experimental time of 15 min. The selectivity towards Au (III) ion of **2** under these optimal conditions make it prospective candidates for chemical sensors or optical materials.

REFERENCES

- [1] Greenwood, N. and Earnshaw, A. Chemistry of the Elements. 2 ed.: Oxford: Butterworth Heinemann, 2001.
- [2] Hashmi, A.S.K. and Hutchings, G.J. Gold Catalysis. Angewandte Chemie International Edition 45(47) (2006): 7896-7936.
- [3] Hashmi, A.S.K. Gold-Catalyzed Organic Reactions. Chemical Reviews 107(7) (2007): 3180-3211.
- [4] Arcadi, A. Alternative Synthetic Methods through New Developments in Catalysis by Gold. Chemical Reviews 108(8) (2008): 3266-3325.
- [5] Della Pina, C., Falletta, E., Prati, L., and Rossi, M. Selective oxidation using gold. Chemical Society Reviews 37(9) (2008): 2077-2095.
- [6] Hashmi, A.S.K. and Rudolph, M. Gold catalysis in total synthesis. Chemical Society Reviews 37(9) (2008): 1766-1775.
- [7] Jiménez-Núñez, E. and Echavarren, A.M. Gold-Catalyzed Cycloisomerizations of Enynes: A Mechanistic Perspective. Chemical Reviews 108(8) (2008): 3326-3350.
- [8] Li, Z., Brouwer, C., and He, C. Gold-Catalyzed Organic Transformations. Chemical Reviews 108(8) (2008): 3239-3265.
- [9] Gorin, D.J. and Toste, F.D. Relativistic effects in homogeneous gold catalysis. Nature 446(7134) (2007): 9.
- [10] Wilson, R. The use of gold nanoparticles in diagnostics and detection. Chemical Society Reviews 37(9) (2008): 2028-2045.
- [11] Saha, K., Agasti, S.S., Kim, C., Li, X., and Rotello, V.M. Gold Nanoparticles in Chemical and Biological Sensing. Chemical Reviews 112(5) (2012): 2739-2779.
- [12] Al-Sa'ady, A.K.H., Moss, K., McAuliffe, C.A., and Parish, R.V. Mossbauer and nuclear magnetic resonance spectroscopic studies on 'Myocrisin', 'Solganol', 'Auranofin', and related gold(I) thiolates. Journal of the Chemical Society, Dalton Transactions (8) (1984): 1609-1616.

- [13] JONES, J.R.E. A Further Study of the Relation Between Toxicity and Solution Pressure, with Polycelis Nigra as Test Animal. Journal of Experimental Biology 17(4) (1940): 408-415.
- [14] BLOCK, W.D. and KNAPP, E.L. METABOLISM, TOXICITY, AND MANNER OF ACTION OF GOLD COMPOUNDS IN THE TREATMENT OF ARTHRITIS: VII. THE EFFECT OF VARIOUS GOLD COMPOUNDS ON THE OXYGEN CONSUMPTION OF RAT TISSUES. Journal of Pharmacology and Experimental Therapeutics 83(4) (1945): 275-278.
- [15] Lee, M.-T., Ahmed, T., and Friedman, M.E. Inhibition of Hydrolytic Enzymes by Gold Compounds I. β -Glucuronidase and Acid Phosphatase by Sodium Tetrachloroaurate (III) and Potassium Tetrabromoaurate (III). Journal of Enzyme Inhibition and Medicinal Chemistry 3(1) (1989): 23-33.
- [16] Habib, A. and Tabata, M. Oxidative DNA damage induced by HEPES (2-[4-(2-hydroxyethyl)-1-piperazinyl]ethanesulfonic acid) buffer in the presence of Au(III). Journal of Inorganic Biochemistry 98(11) (2004): 1696-1702.
- [17] Nyarko, E., et al. In vitro toxicity of palladium(II) and gold(III) porphyrins and their aqueous metal ion counterparts on Trypanosoma brucei brucei growth. Chemico-Biological Interactions 148(1-2) (2004): 19-25.
- [18] Rocha, A., Zhou, Y., Kundu, S., Gonzalez, J., BradleighVinson, S., and Liang, H. In vivo observation of gold nanoparticles in the central nervous system of Blaberus discoidalis. Journal of Nanobiotechnology 9(1) (2011): 5.
- [19] Brian R. Eggins. Chemical Sensors and Biosensors. New York: John Wiley & Sons, 2002.
- [20] Anthony W. Czarnik. Fluorescent Chemosensors for Ion and Molecule Recognition. Vol. 538. Washington DC,: American Chemical Society, 1993.
- [21] Fan, L.-J., et al. Fluorescent conjugated polymer molecular wire chemosensors for transition metal ion recognition and signaling. Coordination Chemistry Reviews 253(3-4) (2009): 410-422.

- [22] Joseph R. Lakowicz. Principles of Fluorescence Spectroscopy. 3rd ed. New York: Springer, 2006.
- [23] Williams, A.T.R., Winfield, S.A., and Miller, J.N. Relative fluorescence quantum yields using a computer-controlled luminescence spectrometer. Analyst 108(1290) (1983): 1067-1071.
- [24] Yang, Y., Yin, C., Huo, F., and Chao, J. A selective fluorescent probe for detection of gold(III) ions and its application to bioimaging. RSC Advances 3(25) (2013): 9637-9640.
- [25] Wang, J.-B., Wu, Q.-Q., Min, Y.-Z., Liu, Y.-Z., and Song, Q.-H. A novel fluorescent probe for Au(III)/Au(I) ions based on an intramolecular hydroamination of a Bodipy derivative and its application to bioimaging. Chemical Communications 48(5) (2012): 744-746.
- [26] Patil, N.T., et al. Exploiting the higher alkynophilicity of Au-species: development of a highly selective fluorescent probe for gold ions. Chemical Communications 48(91) (2012): 11229-11231.
- [27] Park, J.E., Choi, M.G., and Chang, S.-K. Colorimetric and Fluorescent Signaling of Au³⁺ by Desulfurization of Thiocoumarin. Inorganic Chemistry 51(5) (2012): 2880-2884.
- [28] Wang, J., Lin, W., Yuan, L., Song, J., and Gao, W. Development of a reversible fluorescent gold sensor with high selectivity. Chemical Communications 47(46) (2011): 12506-12508.
- [29] Dong, M., Wang, Y.-W., and Peng, Y. Highly Selective Ratiometric Fluorescent Sensing for Hg²⁺ and Au³⁺, Respectively, in Aqueous Media. Organic Letters 12(22) (2010): 5310-5313.
- [30] Grabchev, I., Moneva, I., Bojinov, V., and Guittonneau, S. Synthesis and properties of fluorescent 1,8-naphthalimide dyes for application in liquid crystal displays. Journal of Materials Chemistry 10(6) (2000): 1291-1296.

- [31] Bojinov, V., Ivanova, G., and Simeonov, D. Synthesis and Photophysical Investigations of Novel Polymerizable Blue Emitting Fluorophores – Combination of a Hindered Amine with a Benzo[de]isoquinoline-1,3-dione. Macromolecular Chemistry and Physics 205(9) (2004): 1259-1268.
- [32] Duke, R.M., Veale, E.B., Pfeffer, F.M., Kruger, P.E., and Gunnlaugsson, T. Colorimetric and fluorescent anion sensors: an overview of recent developments in the use of 1,8-naphthalimide-based chemosensors. Chemical Society Reviews 39(10) (2010): 3936-3953.
- [33] Nandhikonda, P., Begaye, M.P., Cao, Z., and Heagy, M.D. Frontier molecular orbital analysis of dual fluorescent dyes: predicting two-color emission in N-Aryl -1,8-naphthalimides. Organic & Biomolecular Chemistry 8(14) (2010): 3195-3201.
- [34] Wang, H., Wu, H., Xue, L., Shi, Y., and Li, X. A naphthalimide fluorophore with efficient intramolecular PET and ICT Processes: Application in molecular logic. Organic & Biomolecular Chemistry 9(15) (2011): 5436-5444.
- [35] Banerjee, S., et al. Recent advances in the development of 1,8-naphthalimide based DNA targeting binders, anticancer and fluorescent cellular imaging agents. Chemical Society Reviews 42(4) (2013): 1601-1618.
- [36] Georgiev, N.I. and Bojinov, V.B. Design, synthesis and sensor activity of a highly photostable blue emitting 1,8-naphthalimide. Journal of Luminescence 132(9) (2012): 2235-2241.
- [37] Bojinov, V. and Grabchev, I. A new method for synthesis of 4-allyloxy-1,8-naphthalimide derivatives for use as fluorescent brighteners. Dyes and Pigments 51(1) (2001): 57-61.
- [38] Grabchev, I., Petkov, C., and Bojinov, V. 1,8-Naphthalimides as Blue Emitting Fluorophores for Polymer Materials. Macromolecular Materials and Engineering 287(12) (2002): 904-908.
- [39] Grabchev, I., Staneva, D., Dumas, S., and Chovelon, J.-M. Metal ions and protons sensing properties of new fluorescent 4-N-methylpiperazine-1,8-naphthalimide

- terminated poly(propyleneamine) dendrimer. Journal of Molecular Structure 999(1–3) (2011): 16-21.
- [40] Yu, C., et al. “Off-On” based fluorescent chemosensor for Cu²⁺ in aqueous media and living cells. Talanta 85(3) (2011): 1627-1633.
- [41] Dai, H. and Xu, H. A water-soluble 1,8-naphthalimide-based ‘turn on’ fluorescent chemosensor for selective and sensitive recognition of mercury ion in water. Bioorganic & Medicinal Chemistry Letters 21(18) (2011): 5141-5144.
- [42] Wang, J., Yang, L., Hou, C., and Cao, H. A new N-imidazolyl-1,8-naphthalimide based fluorescence sensor for fluoride detection. Organic & Biomolecular Chemistry 10(31) (2012): 6271-6274.
- [43] Zhang, C., Liu, Z., Li, Y., He, W., Gao, X., and Guo, Z. In vitro and in vivo imaging application of a 1,8-naphthalimide-derived Zn²⁺ fluorescent sensor with nuclear envelope penetrability. Chemical Communications 49(97) (2013): 11430-11432.
- [44] Dai, L.-X., Tu, T., You, S.-L., Deng, W.-P., and Hou, X.-L. Asymmetric Catalysis with Chiral Ferrocene Ligands. Accounts of Chemical Research 36(9) (2003): 659-667.
- [45] Bolm, C., Muñoz-Fernández, K., Seger, A., Raabe, G., and Günther, K. On the Role of Planar Chirality in Asymmetric Catalysis: A Study toward Appropriate Ferrocene Ligands for Diethylzinc Additionst. The Journal of Organic Chemistry 63(22) (1998): 7860-7867.
- [46] Imahori, H., et al. Stepwise Charge Separation and Charge Recombination in Ferrocene-meso,meso-Linked Porphyrin Dimer–Fullerene Triad. Journal of the American Chemical Society 124(18) (2002): 5165-5174.
- [47] Ding, J., Feng, K., Tung, C.-H., and Wu, L.-Z. Long-Lived Charge Separation in a Dyad System Containing Cyclometalated Platinum(II) Complex and Ferrocene Donor. The Journal of Physical Chemistry C 115(3) (2010): 833-839.
- [48] Maeda, D., Shimakoshi, H., Abe, M., Fujitsuka, M., Majima, T., and Hisaeda, Y. Synthesis of a Novel Sn(IV) Porphycene–Ferrocene Triad Linked by Axial

- Coordination and Solvent Polarity Effect in Photoinduced Charge Separation Process. Inorganic Chemistry 49(6) (2010): 2872-2880.
- [49] Supur, M., El-Khouly, M.E., Seok, J.H., Kay, K.-Y., and Fukuzumi, S. Elongation of Lifetime of the Charge-Separated State of Ferrocene–Naphthalenediimide–[60]Fullerene Triad via Stepwise Electron Transfer. The Journal of Physical Chemistry A 115(50) (2011): 14430-14437.
- [50] Li, F., Pandey, B., and Ito, T. Linker-Based Control of Electron Propagation through Ferrocene Moieties Covalently Anchored onto Insulator-Based Nanopores Derived from a Polystyrene–Poly(methylmethacrylate) Diblock Copolymer. Langmuir 28(48) (2012): 16496-16500.
- [51] Fery-Forgues, S. and Delavaux-Nicot, B. Ferrocene and ferrocenyl derivatives in luminescent systems. Journal of Photochemistry and Photobiology A: Chemistry 132(3) (2000): 137-159.
- [52] Cao, W., Ferrance, J.P., Demas, J., and Landers, J.P. Quenching of the Electrochemiluminescence of Tris(2,2'-bipyridine)ruthenium(II) by Ferrocene and Its Potential Application to Quantitative DNA Detection. Journal of the American Chemical Society 128(23) (2006): 7572-7578.
- [53] Zhang, R., Wang, Z., Wu, Y., Fu, H., and Yao, J. A Novel Redox-Fluorescence Switch Based on a Triad Containing Ferrocene and Perylene Diimide Units. Organic Letters 10(14) (2008): 3065-3068.
- [54] Caballero, A., et al. Selective Fluorescence Sensing of Li⁺ in an Aqueous Environment by a Ferrocene–Anthracene-Linked Dyad. Organic Letters 6(24) (2004): 4599-4602.
- [55] Deng, S., Lei, J., Liu, Y., Huang, Y., and Ju, H. A ferrocenyl-terminated dendrimer as an efficient quencher via electron and energy transfer for cathodic electrochemiluminescent bioanalysis. Chemical Communications 49(21) (2013): 2106-2108.

- [56] Gan, J., et al. Synthesis and luminescence properties of novel ferrocene–naphthalimides dyads. Journal of Organometallic Chemistry 645(1–2) (2002): 168–175.
- [57] McAdam, C.J., Robinson, B.H., Simpson, J., and Tagg, T. Ferrocenyl–Naphthalimide Donor–Acceptor Dyads with Aromatic Spacer Groups. Organometallics 29(11) (2010): 2474–2483.
- [58] Chen, S., Lu, J., Sun, C., and Ma, H. A highly specific ferrocene-based fluorescent probe for hypochlorous acid and its application to cell imaging. Analyst 135(3) (2010): 577–582.
- [59] Philipova, T. and Petkov, I. Synthesis, spectral properties, and application of 1,8-naphthalimide fluorophores for modified polymers. Journal of Applied Polymer Science 80(11) (2001): 1863–1869.
- [60] Benanti, T.L., Saejueng, P., and Venkataraman, D. Segregated assemblies in bridged electron-rich and electron-poor [small pi]-conjugated moieties. Chemical Communications (7) (2007): 692–694.
- [61] Chatterjee, A., et al. Selective Fluorogenic and Chromogenic Probe for Detection of Silver Ions and Silver Nanoparticles in Aqueous Media. Journal of the American Chemical Society 131(6) (2009): 2040–2041.
- [62] Baathulaa, K., Xu, Y., and Qian, X. Unusual large Stokes shift and solvatochromic fluorophore: Synthesis, spectra, and solvent effect of 6-substituted 2,3-naphthalimide. Journal of Photochemistry and Photobiology A: Chemistry 216(1) (2010): 24–34.
- [63] Marinova, N.V., Georgiev, N.I., and Bojinov, V.B. Design, synthesis and pH sensing properties of novel 1,8-naphthalimide-based bichromophoric system. Journal of Photochemistry and Photobiology A: Chemistry 222(1) (2011): 132–140.
- [64] Sirilaksanapong, S., Sukwattanasinitt, M., and Rashatasakhon, P. 1,3,5-Triphenylbenzene fluorophore as a selective Cu²⁺ sensor in aqueous media. Chemical Communications 48(2) (2012): 293–295.

- [65] Thongmalai, W., et al. Polydiacetylenes carrying amino groups for colorimetric detection and identification of anionic surfactants. Journal of Materials Chemistry 21(41) (2011): 16391-16397.
- [66] Yuanboonlim, W., Siripornnoppakhun, W., Niamnont, N., Rashatasakhon, P., Vilaivan, T., and Sukwattanasinitt, M. Phenylene–ethynylene trication as an efficient fluorescent signal transducer in an aptasensor for potassium ion. Biosensors and Bioelectronics 33(1) (2012): 17-22.
- [67] Vongnam, K., Vilaivan, T., Sukwattanasinitt, M., and Rashatasakhon, P. New Water Soluble Terphenylene Diethynylene Fluorophores. Journal of Fluorescence 24(1) (2014): 197-202.
- [68] Jung Jou, M., et al. Highly selective fluorescent probe for Au³⁺ based on cyclization of propargylamide. Chemical Communications (46) (2009): 7218-7220.
- [69] Yamamoto, H., Sasaki, I., Imagawa, H., and Nishizawa, M. Hg(OAc)₂·0.1Sc(OTf)₃-Catalyzed Cycloisomerization of 2-(4-Pentynyl)furan. Organic Letters 9(7) (2007): 1399-1402.



APPENDIX

จุฬาลงกรณ์มหาวิทยาลัย
CHULALONGKORN UNIVERSITY

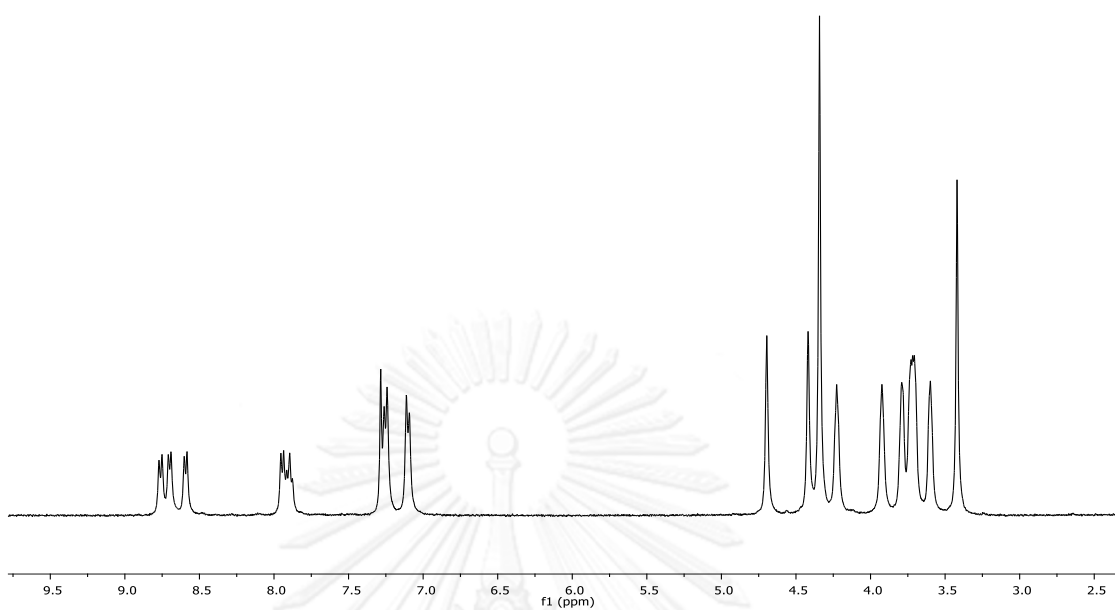


Figure A.1 $^1\text{H-NMR}$ (400 MHz) of compound 1 in CDCl_3 .

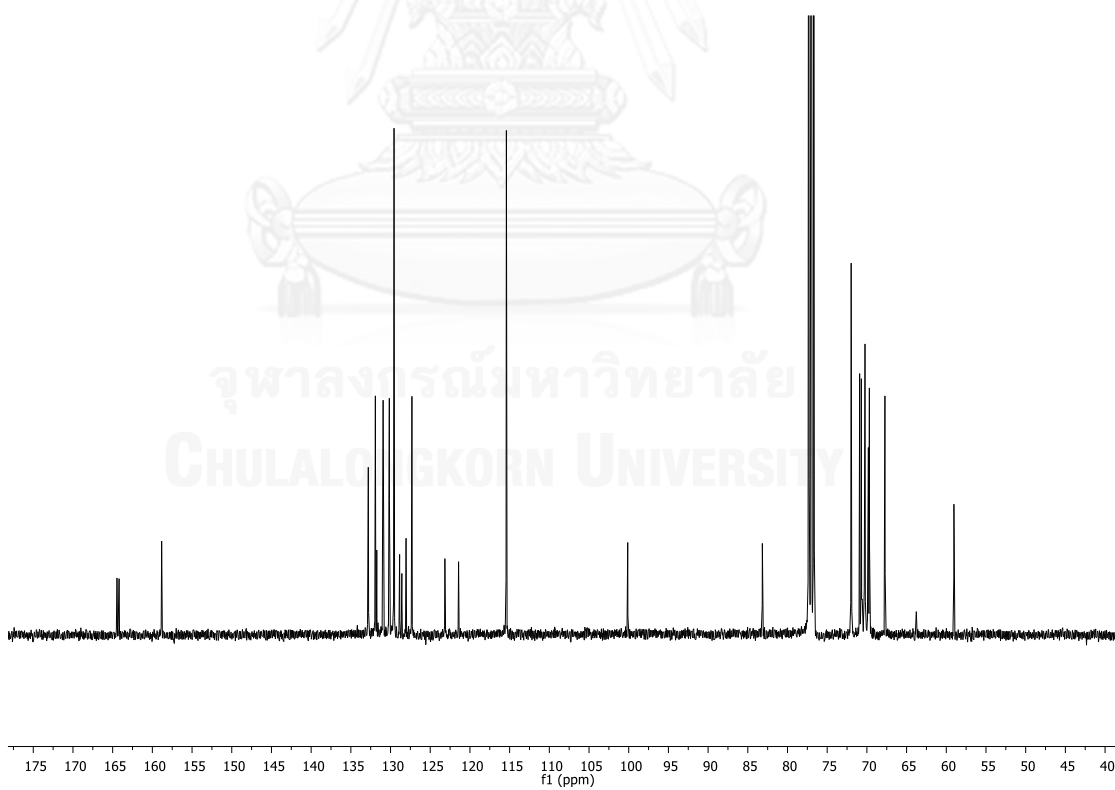


Fig.A.2 $^{13}\text{C-NMR}$ (400 MHz) of compound 1 in CDCl_3

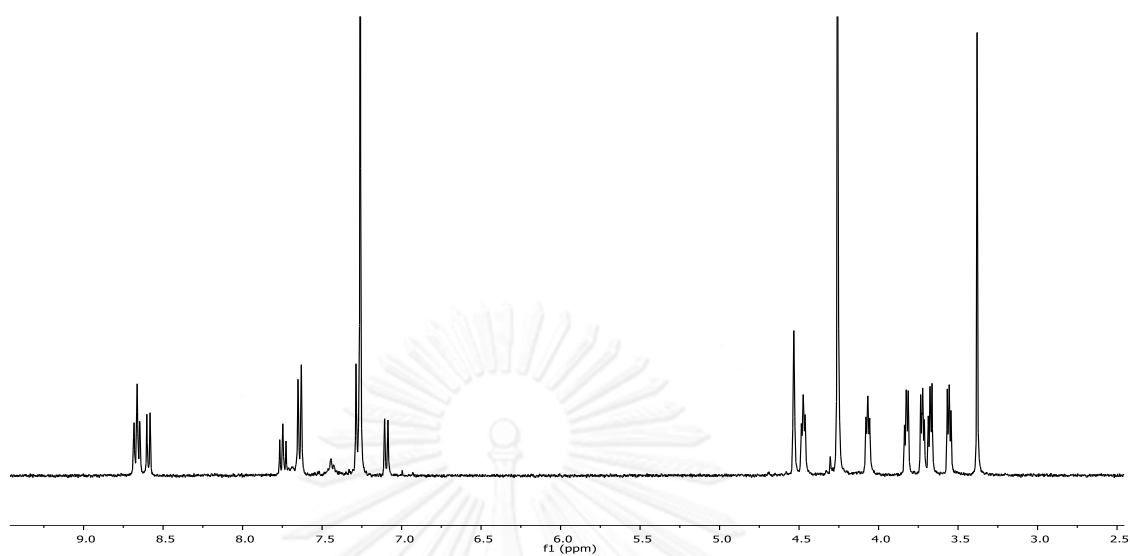


Figure A.3 $^1\text{H-NMR}$ (400 MHz) of compound 2 in CDCl_3 .

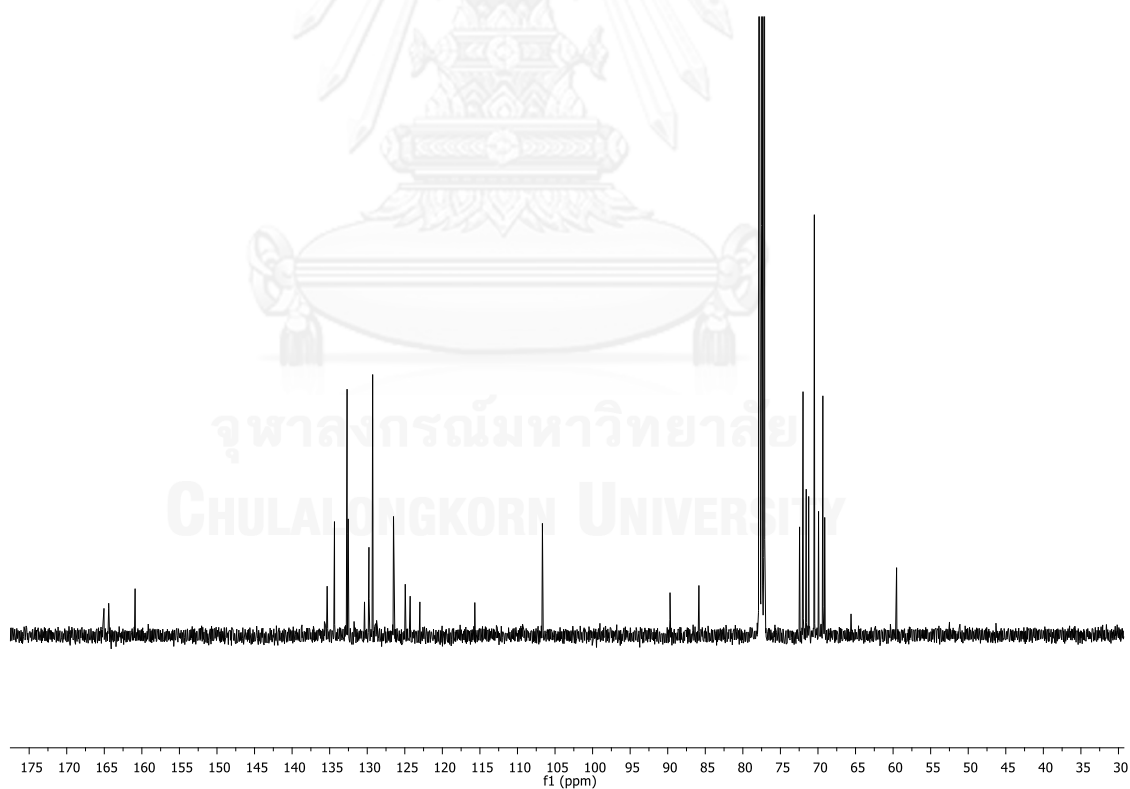


Figure A.4 $^{13}\text{C-NMR}$ (400 MHz) of compound 2 in CDCl_3 .

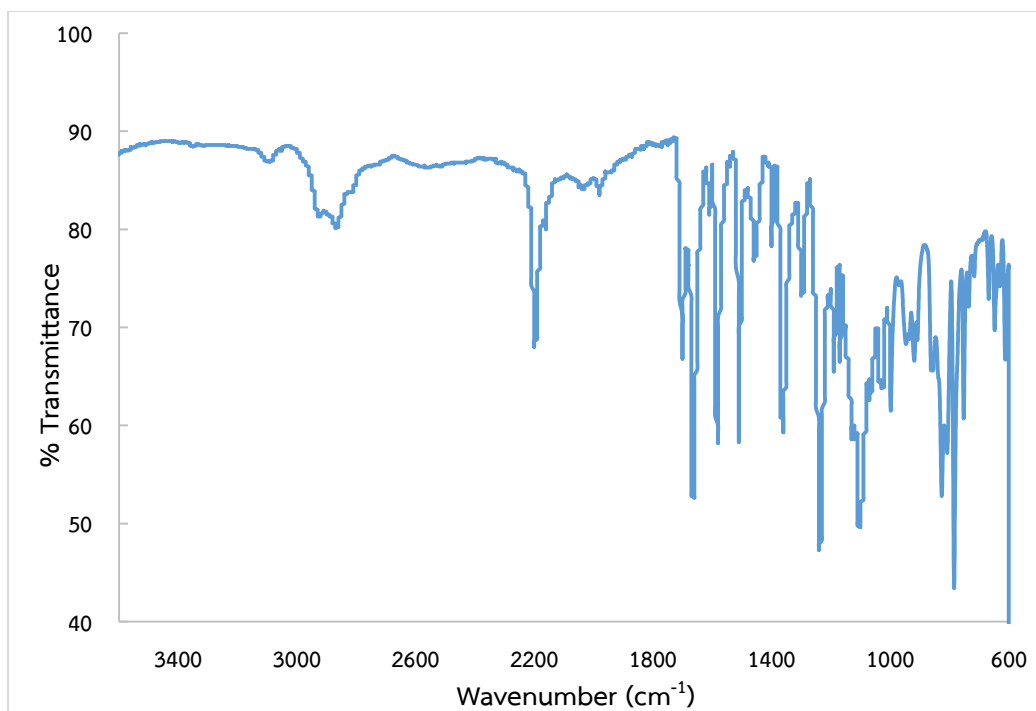


Figure A.5 Infrared spectrum of compound 1 (solid).

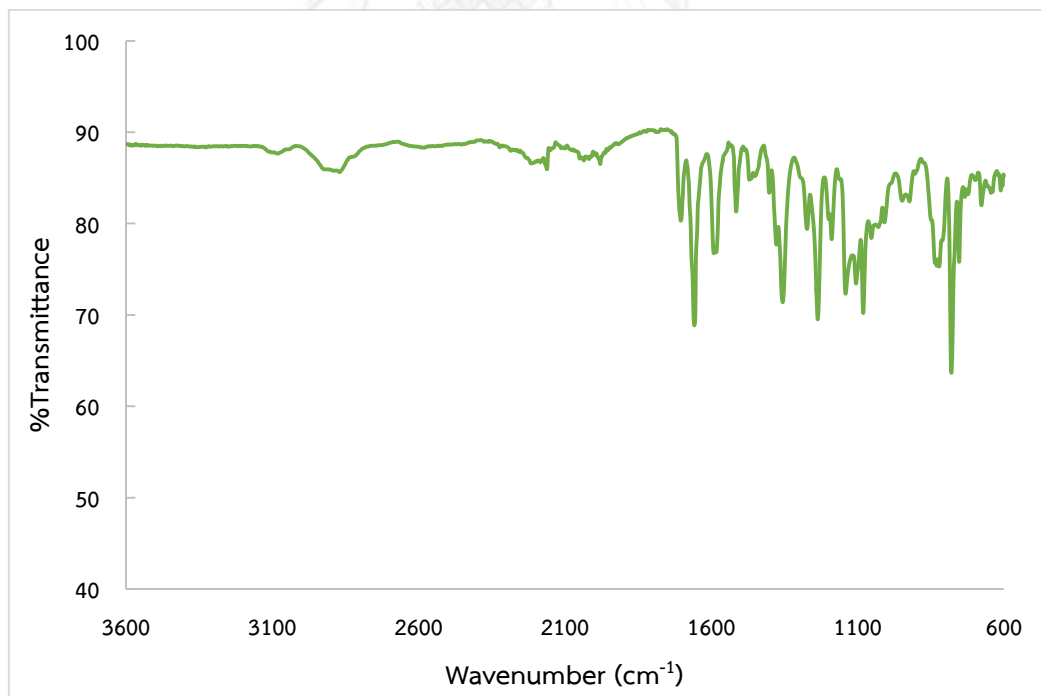
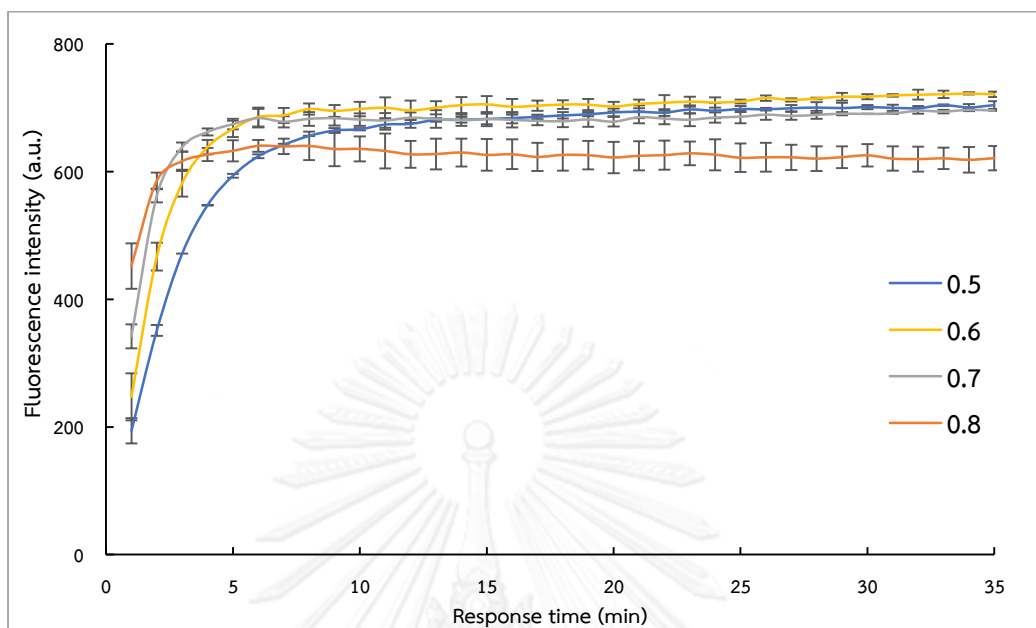


Figure A.6 Infrared spectrum of compound 2 (solid).



[2] = 5 μ M; [Au(III)] = 0.5 mM in CH₃CN-PBS (pH 8.0, 10 mM) (λ_{ex} 369 nm, λ_{em} 456 nm)

Figure A.7 Pre-screening of effect of water content on fluorescence intensity of 2 towards Au(III) in various volume ration of aqueous 0.5 – 0.8.

The structures of compound **1** and **2** optimized using density functional theory (DFT) method at the B3LYP/LANL2DZ level of theory are shown in Figure S1. The B3LYP/LANL2DZ-computed HOMO energies of the compound **1** and **2** are -5.535 and -6.470 eV, respectively. All the computations were performed using GAUSSIAN 09 package program. (Frisch, M. J. et al; Gaussian 09, Revision D.01, Gaussian, Inc., Wallingford CT, 2014.)

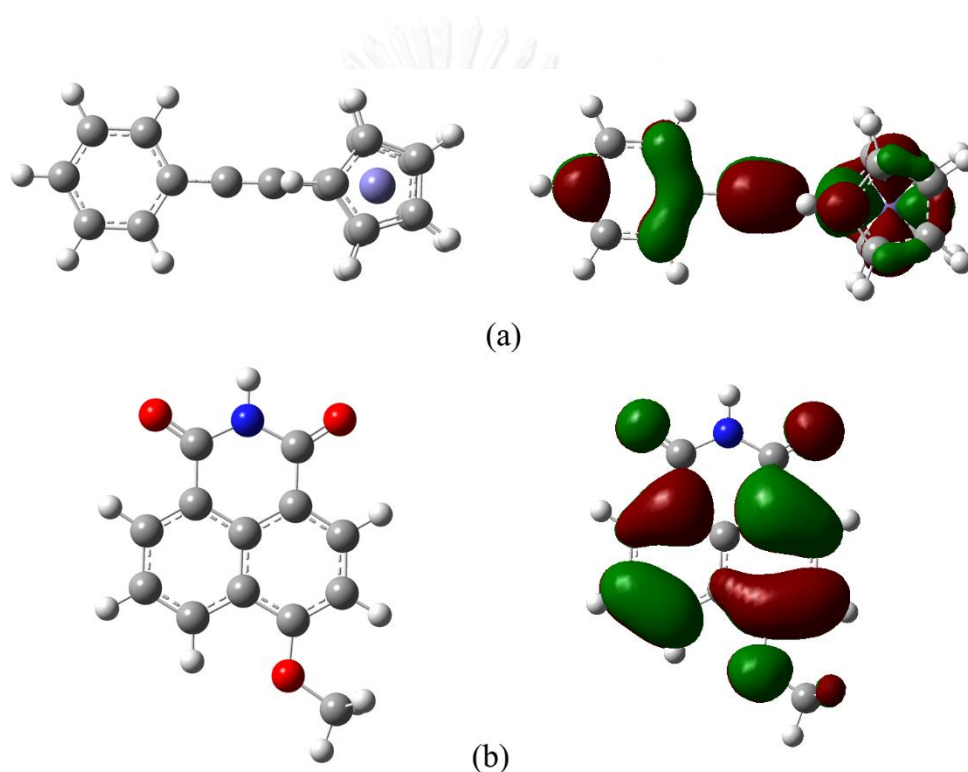


Figure A.8 The B3LYP/LANL2DZ-optimized structures of compound (a) **1** and (b) **2** and their HOMOs illustrated on the right side were plotted at an isovalue of 0.02 e.

VITA

Pondchanok Chinapang received her B.Sc. degree from Chiang Mai University in March 2011 and continues her graduate studied at Department of Chemistry, Faculty of Science, Chulalongkorn University from June 20011, under supervision of Assoc. Prof. Paitoon Rashtasakhon. During her master course, she joined Masaoka's group at Institute for Molecular Science (IMS), Okazaki, Japan as exchange student for 5 months. Her recent research is focus on the design and synthesis of novel fluorescent materials for selective recognition of metal ions.

